This is a preprint, the final version is subject to change, of the American Mineralogist (MSA)
Cite as Authors (Year) Title. American Mineralogist, in press.
(DOI will not work until issue is live.) DOI: http://dx.doi.org/10.2138/am-2016-5718

Revision 1

Temporal histories of Cordilleran continental arcs: testing models for magmatic episodicity

Moritz Kirsch[1]*, Scott R. Paterson[2], Florian Wobbe[3], Ana María Martínez Ardila[4], Benjamin L. Clausen[4], and Pablo H. Alasino[5]

[1] *Institut für Geologie, Technische Universität Bergakademie Freiberg, Bernhard-von-Cotta-Strasse 2, 09599 Freiberg, Germany*

[2] *Department of Earth Sciences, University of Southern California, Los Angeles, CA 90089-0740, U.S.A.*

[3] *Alfred Wegener Institute, Am Alten Hafen 26, 27568 Bremerhaven, Germany*

[4] *Department of Earth and Biological Sciences, Loma Linda University, Griggs Hall, 11065 Campus Street, Loma Linda, California 92350, U.S.A*

[5] *CRILAR-CONICET, Entre Ríos y Mendoza, Anillaco 5301, La Rioja, Argentina*

* Corresponding author; Phone: +49 (0)3731 1680105; Email: moritz.kirsch@geo.tu-freiberg.de

Abstract

Magmatic activity in continental arcs is known to vary in a non-steady state manner, with the mechanisms driving magmatic activity being a matter of ongoing discussion. Of particular importance is the question of what extent episodic magmatism in continental arcs is governed by external factors (e.g., plate motions) and internal factors (e.g., feedback processes in the upper plate). In order to test existing models for magmatic episodicity, which are mostly based on temporally and spatially limited records, this study uses large datasets of geochronological, geochemical, and plate kinematic data to document the Paleozoic to Mesozoic development of the North and South American Cordilleras in eight transects from British Columbia to Patagonia. The temporal distribution of U/Pb bedrock and detrital zircon ages, used as a proxy for timing of magmatic accretion, shows that some minima and maxima of zircon abundance are nearly synchronous for thousands of km along the arc. Some age patterns are characterized by a periodicity of 50–80 Ma, suggesting a cyclic controlling mechanism. Other magmatic lulls or flare-ups find no equivalents in adjacent sectors, indicating that either discrete events or variable lag times may also be important in governing magmatic activity in continental arcs. Magma composition in Mexico, the Peninsular Ranges, and the Sierra Nevada varies episodically and proportionally with the temporal record of arc activity. During flare-up events, there is an increase in Sm/Yb, indicating deeper melting, and a decrease in εNd_i, suggesting a higher degree of crustal assimilation. Geochemical scatter also increases during the initiation of flare-up events. Plate kinematic data provide a means of evaluating mantle heat input. The correlation between plate convergence rate and magmatic accretion varies for each sector, suggesting that different flare-ups or lulls likely reflect variable combinations of processes.

Keywords: magmatism, continental arc, Cordilleras, geochronology, geochemistry, plate motions, Paleozoic, Mesozoic

Introduction

Convergent continental margins, where oceanic lithosphere is subducted beneath continental lithosphere, are areas of intense magmatism, and important sites of crustal growth (e.g., Crisp 1984; Rudnick 1995; Tatsumi 2005; Davidson and Arculus 2006). Assessing crustal production rates and understanding the mechanisms controlling magmatic addition in continental arcs are two issues that are of key importance in tectonic studies (e.g., Ducea et al. 2015; Jicha and Jagoutz 2015). The Cordilleran orogenic system of North and South America is particularly well suited for addressing these aspects, as it features a spatially extensive (>15,000 km), nearly continuous mountain belt that is the expression of subduction of oceanic lithosphere beneath a continental margin. Subduction-related activity in the American Cordilleras was initiated in the Early Paleozoic along some parts of the arc (e.g., Bahlburg and Hervé 1997; Ramos 2009) and is still on-going today, providing an exceptionally long continental magmatic arc record. Based on the relative abundance of igneous rocks with known ages, a non-steady state behavior of magmatic arc activity, characterized by periods of reduced magmatism alternating with magmatic flare-ups, has been documented in several Cordilleran arc segments. These include the Coastal Ranges, British Colombia (e.g., Armstrong 1988; Ducea and Barton 2007; Gehrels et al. 2009), the Cascade Mountains, Washington (Miller et al. 2009), the Sierra Nevada, California (Bateman and Shervais 1992; Ducea 2001; DeCelles et al. 2009; Paterson et al. 2014), the Transverse Ranges, California (Barth et al. 1997; 2008), the Salinian arc (Kidder et al. 2003; Ducea et al. 2003; Chapman et al. 2014), the Peninsular Ranges Batholith (Premo et al. 2014), the Sierra Madre Occidental and Trans-Mexican Volcanic Belt, Mexico (Ferrari et al. 1999), and the central Andes (Haschke 2002; Haschke et al. 2006; Trumbull et al. 2006).

Existing models to explain the non-steady state magmatic activity of continental arcs either invoke (i) external forcing by plate tectonic processes (Pilger 1984; Hughes and Mahood 2008), (ii) intra-arc cyclic processes largely independent of plate motions (Kay and Mahlburg Kay 1993; Ducea and Barton 2007; DeCelles et al. 2009; Lee et al. 2013) or (iii) a crustal modulation of mantle energy input (de Silva and Gosnold 2007; de Silva 2008; de Silva et al. 2015). Most of these models are based on a temporally and spatially limited record. In order to test the validity of the proposed models, large datasets are needed.

This paper uses an ever-growing database of U-Pb bedrock and detrital zircon age data between 400 and 80 Ma for the American Cordilleras from British Colombia in the north to Patagonia in the south as a means to evaluate the timing and relative strength of continental arc magmatic activity. As the proposed mechanisms for magmatic arc activity operate over distinct temporal and spatial scales, evaluating the scale of repeated age patterns provides a means to test these proposals. Furthermore, by examining 15,000 km of arc length, we are able to evaluate if the proposed mechanisms invoked for a small segment of an arc are representative for entire arc systems, which exhibit variable basement characteristics and subducting plate parameters.

A fundamental question concerns the role of external factors (e.g. plate motions and mantle power) vs. internal factors (e.g. feedback processes in the upper plate) in controlling continental arc magmatic activity. To assess the relative importance of these respective factors, this study evaluates the spatial and temporal pattern of magmatic arc activity as well as the relationship between magmatic accretion rate and (i) plate kinematic parameters such as plate convergence rate that control magma production in the mantle wedge (e.g., Cagnioncle et al. 2007), and (ii) arc magma composition, which is primarily governed by processes during the transfer of magma from the mantle wedge to the upper crust, i.e. it depends on thickness, composition, and state of stress of the upper plate (e.g., Leeman 1983; Mantle and Collins 2008; Chiaradia 2015).

Geological setting

The North American Cordilleras and the Andes (henceforth collectively referred to as "Cordilleras", "Cordilleran orogen", "Cordilleran arc", or "Cordilleran margin") extend along the western edge of the North and South American continents, respectively, and together form a long (ca. 15,000 km), nearly continuous belt of magmatic arc assemblages generated by the persistent convergence and interaction between lower oceanic and upper continental plates (Dewey and Bird 1970; e.g., Dickinson 1970; Armstrong 1974). Following the break-up of Rodinia, subduction along the North American Cordilleran margin initiated in the Middle–Late Devonian (Burchfiel and Davis 1972; 1975; Monger and Price 2002; Dickinson 2004; 2009), whereas the western margin of South America preserves a record of almost continuous subduction since the Cambrian, with the inception of the Terra Australis orogen (Rapela et al. 1998a; 1998b; Pankhurst et al. 2000; Ramos and Aleman 2000; Cawood 2005; Chew et al. 2007; Collo et al. 2009). Despite having formed under one geodynamic regime, the Cordilleran orogen is segmented, i.e. features along-strike tectonic, structural, and morphological variations (Sempere et al. 2008; Ramos 2009). For the sake of the analysis in this paper, the Cordilleran margin is divided into eight sectors, from north (British Colombia) to south (Patagonia): (1) the Coast Ranges, (2) the Sierra Nevada, (3) the Peninsular Ranges to Mojave, (4) southeastern Mexico and Central America, (5) the northern Andes, (6) the Peruvian Andes, (7) the south-central Andes, and (8) the southern Andes. In some cases, the boundaries of these sectors coincide with the spatial limits of tectono-magmatic provinces. In other cases the division is arbitrary and simply a matter of choosing sectors large enough to incorporate a statistically meaningful amount of data, and small enough to account for local differences in the geological evolution. In the following sections, the tectonic and magmatic history of the individual Cordilleran arc sectors are briefly summarized. Age compilations and analyses of arc processes presented in this paper are limited to a timeframe between 400 and 80 Ma, hence these summaries focus on the late

Paleozoic and early Mesozoic geological history, with particular emphasis on subduction initiation and evolution.

Coast Ranges (55–43° N)

The most northern sector is defined as the region between 55 and 43° N and includes magmatic activity in British Columbia, Washington, Oregon, Idaho, and Montana. The pre-Cretaceous geological history of this region includes the accretion of several oceanic arc terranes, such as the Stikinia, Quesnellia, Wrangellia and Triassic Chelan Mountains terrane (Tabor et al. 1989; Miller et al. 1994; Matzel et al. 2004). Subsequent continental arc magmatism in this region is preserved in the ca. 1500 km long Coast Plutonic Complex (e.g., Monger et al. 1982; Tabor et al. 1989), which records continental magmatic arc activity between ca. 170 and ca. 50 Ma with flare-ups at 160–140 Ma, 120–78 Ma, and 55–48 Ma (Gehrels et al. 2009). Magmatism was accompanied by crustal extension until the mid-Cretaceous, when the accretion of the Alexander-Wrangellia terrane to the western margin of Laurentia caused local contraction, crustal thickening and thrusting (Gehrels et al. 2009). The Late Cretaceous to Early Tertiary marks a transition to dextral transpressional tectonics in the Coast Mountains sector, attributed to changing plate kinematics, which resulted in a dramatic reduction of magmatic production (Gehrels et al. 2009). During the Late Cretaceous to Early Tertiary, arc magmatism in the Coast Mountains Batholith migrated eastward. From ca. 50 Ma onwards, the temporal and spatial evolution as well as the geochemical characteristics of arc magmatism within the forearc areas from Alaska to Oregon are complex due to the interaction of several spreading ridges and oceanic transforms with the subduction zone (Haeussler et al. 2003; Madsen et al. 2006; du Bray and John 2011).

Sierra Nevada (43–35° N)

The Sierra Nevada section of the Cordilleran magmatic arc is located in central and eastern California and western Nevada, USA, between approximately 43° N and 35° N (Barton et al. 1988; Bateman 1992; Van Buer et al. 2009; Van Buer and Miller 2010). After the breakup of Rodinia in the Late Neoproterozoic, this part of the Cordilleran margin remained passive until the middle to late Devonian, when an intraoceanic arc complex formed in the eastern Klamath and northern Sierra terranes (Bradley 2008; Dickinson 2009; Colpron and Nelson 2011). These subduction complexes subsequently collided with the Pacific margin during the the Late Devonian to Early Mississippian Antler orogeny, which involved thrusting the Roberts Mountains Allochthon onto Neoproterozoic to Paleozoic miogeoclinal rocks (Schweickert and Cowan 1975; Stevens and Greene 1999; Gehrels et al. 2000; Chapman et al. 2012). Late Devonian to Early Carboniferous extensional tectonics that gave rise to a marginal ocean basin called the Slide Mountain Ocean Basin (Davis et al. 1978; Nokleberg et al. 2000; Nelson et al. 2006; Saleeby and Dunne 2015). This ocean basin closed in the Middle Permian as a consequence of a subduction zone jump and polarity reversal, which led to the accretion of additional fringing oceanic island arc complexes (e.g., the Golconda Allochthon) onto the Laurentian platform during the Late Permian–Early Triassic Sonoma orogeny (Riley et al. 2000; Dickinson 2009). The Early Triassic marks the inception of a continental magmatic arc along the Sierran sector of the Cordilleran orogen (Barth and Wooden 2006; Paterson et al. 2014). Continued subduction of Pacific lithosphere culminated in the construction of the voluminous Sierra Nevada batholith, which records episodic magmatic activity between ca. 250 and ca. 80 Ma with peaks occurring in Triassic (ca.

230–210 Ma), Middle to Late Jurassic (ca. 180–160 Ma), and mid-Cretaceous (ca. 115–85 Ma) time (Stern et al. 1981; Ducea and Barton 2007; Ducea 2011; Paterson et al. 2014). Latest Cretaceous pluton crystallization ages become progressively younger towards the east, which has been associated with gradual slab flattening (Chen and Moore 1982; Silver and Chappell 1988). The ensuing episode of flat-slab subduction is commonly linked with the Laramide orogeny (Dickinson and Snyder 1978; Miller et al. 1992; Saleeby 2003), and eventually led to the cessation of magmatism in the Sierras at ca. 85 Ma (Chen and Moore 1982; Lipman 1992).

Peninsular and Transverse Ranges, Mojave, and northern Mexico (35–20° N)

This sector extends from the southern limit of the Sierra Nevada at approximately 35° N to about 20° N, and includes the morphotectonic domains of the Peninsular Ranges, Transverse Ranges, Mojave Desert and restored batholithic rocks in Salinia in the US as well as Baja California and the Cordillera Occidental in Mexico. The plutonic record of this region includes overlapping continental arc segments of Permian to Cretaceous age (Barth et al. 2008). Mesozoic (Triassic to Cretaceous) plutonic suites are distributed in this region along three NNW-trending belts (Barth et al. 1997; Kistler et al. 2014). Early to Late Cretaceous magmatism is manifested by the numerous plutons of the ca. 128–86 Ma Peninsular Ranges Batholith that records a west to east progression of subduction transitioning from an oceanic to a continental arc setting (Morton et al. 2014; Hildebrand and Whalen 2014b).

Southeastern Mexico and Central America (25–15° N)

Southeastern Mexico and Central America are composed of several fault-bounded crustal

This is a preprint, the final version is subject to change, of the American Mineralogist (MSA)
Cite as Authors (Year) Title. American Mineralogist, in press.
(DOI will not work until issue is live.) DOI: http://dx.doi.org/10.2138/am-2016-5718

blocks with different geological histories. These blocks were juxtaposed in the course of Pangea amalgamation and dispersal in the Paleozoic and Mesozoic (Campa and Coney 1983; Sedlock et al. 1993; Dickinson and Lawton 2001; Keppie 2004). Processes attributed to the subduction of (Paleo-)Pacific oceanic lithosphere have affected the region at least since the Carboniferous (Proenza et al. 2004; Keppie et al. 2008; 2010; 2012; Galaz et al. 2013). Continental arc magmatism was particularly abundant during the Carboniferous–Permian, as suggested by the detrital zircon record and an abundance of Carboniferous–Permian igneous rocks in the Mixteca and Oaxaquia terranes (Torres et al. 1999; Kirsch et al. 2012; Ortega-Obregón et al. 2014) as well as the Chiapas Massif of the Maya block (Schaaf et al. 2002; Weber et al. 2007; Solari et al. 2009). In the Acatlán Complex, which forms the Paleozoic basement of the Mixteca terrane, basin formation and the intrusion of calc-alkaline plutons was associated with local intra-arc extension, interpreted as a result of oblique, east dipping Pacific subduction (Ramos-Arias et al. 2008; Keppie et al. 2012; Kirsch et al. 2013). The Middle–Late Triassic history of southeastern Mexico is characterized by subdued magmatic arc activity and local shortening and uplift, which have been attributed to transient flat-slab subduction (Kirsch et al. 2014). Magmatic arc activity was re-established by the Early–Middle Jurassic and continued into the Cretaceous (e.g., Barboza-Gudiño et al. 2004; Campa-Uranda et al. 2004; Fastovsky et al. 2005; Barboza-Gudiño et al. 2008; Zavala-Monsiváis et al. 2009; Godínez-Urban et al. 2011; Zavala-Monsiváis et al. 2012). During the Late Triassic to Early Jurassic, peripheral (back-arc?) ocean basins formed at the western margin of continental Mexico (Centeno-García et al. 1993; Martini et al. 2010), accompanied by the deposition of siliciclastic rocks with a passive margin signature (Silva-Romo et al. 2000;

Centeno-García 2005) and the intrusion of mafic rocks with a back-arc geochemical signature (Grajales-Nishimura et al. 1999; Valencia-Moreno et al. 2001; Keppie et al. 2006; Helbig et al. 2012a; 2012b). These basins were subsequently closed in the Early Cretaceous, when a Middle Jurassic–Lower Cretaceous arc assemblage known as the Guerrero Composite Terrane accreted to mainland Mexico (Martini et al. 2011; 2013; Palacios-García and Martini 2014).

Northern Andes (12° N–5° S)

The sector referred to as the Northern Andes comprises the western margin of South America between 12° N and 5° S, i.e. Colombia and Ecuador, and western Venezuela. The southern boundary of this sector coincides with the Huancabanga deflection, which marks a change in strike orientation of the Andean orogen. Due to the paleogeographical location of this region (i.e. proximal to the Ouachita-Marathon suture), the Paleozoic to Mesozoic tectonic and magmatic history of the Northern Andes, recently summarized by Spikings et al. (2014), is to a large part influenced by processes related to Pangea assembly and break-up. The earliest evidence of a continental arc in the northern Andes includes arc-derived Ordovician schists and gneisses in the Eastern Cordillera of Ecuador and the Central Cordillera of Colombia (Litherland et al. 1994; Carmona and Pimentel 2002; Chew et al. 2007). Magmatic rocks of age 290–240 Ma occur in the Santa Marta Massif and the Guajira Peninsula, as well as in the Cordillera Central in Colombia (Litherland et al. 1994; Cardona et al. 2010; Villagómez et al. 2011; Laya and Tucker 2012; Van der Lelij et al. 2016) and are interpreted to have formed above an east dipping Pacific subduction zone during the final stages of Pangea formation. Based on plate reconstructions (Elías-Herrera and Ortega-Gutiérrez 2002; Weber et al. 2007) and the occurrence of similarly aged arc-related igneous rocks, the basement terranes of southern Mexico and Central America are interpreted to have formed the conjugate margin to NW South America (Cochrane et al. 2014). Crustal anatectites and juvenile mafic suites with ages of 240–216 Ma may record the oblique rifting of these Mexican terranes from the NW South American margin. The ensuing passive margin stage was superseded by renewed active margin magmatism that initiated diachronously along the North Andean margin between 213 and 185 Ma (Cochrane et al. 2014; Van der Lelij et al. 2016) and continued into the Cretaceous (Villagómez et al. 2011; Boekhout et al. 2012; Reitsma 2012; Villagómez and Spikings 2013; Cochrane et al. 2014). A period of back-arc extension marks the period of 145–114 Ma, which led to the emplacement of juvenile igneous rocks in the Cordillera Real, Cordillera Central and the Santander Massif (Litherland et al. 1994; Romeuf et al. 1995; Bustamante et al. 2010; Cochrane et al. 2014; Van der Lelij et al. 2016) and may have resulted in the detachment of continental slivers (Chaucha and Tahamí terranes, Spikings et al. 2014 and references therein). These slivers are inferred to have been accreted back to the margin during a switch to compressional tectonics at ca. 115 Ma (Ruiz et al. 2007; Villagómez et al. 2011). Arc magmatism is scarce between ca. 115 Ma and 100 Ma due to highly oblique convergence between the newly formed Caribbean plate and the South American plate (Pindell and Kennan 2009). The origin of felsic magmatism at 100–75 Ma, e.g. represented by the 95–85 Ma Antioquia batholith (Villagómez et al. 2011; Villagómez and Spikings 2013), is currently debated (Pindell and Kennan 2009; Spikings et al. 2014). Mafic igneous rocks occurring in the Western Cordillera of Ecuador and Colombia that have ages between ca. 100 and 85 Ma belong to the Caribbean Large Igneous Province, parts of which amalgamated to northwestern South America at 75–70 Ma (Spikings et al. 2001; Kerr et al. 2002; Vallejo et al. 2006; Spikings et al. 2010; Villagómez and Spikings 2013).

Peruvian Andes (6–18° S)

In the Peruvian Andes, located between 6° S (the Huancabamba deflection) and 18° S (the Arica deflection, or Bolivian orocline), continental arc magmatism initiated in the Ordovician as part of the Famatinian orogenic cycle (Mukasa and Henry 1990; Gosen and Prozzi 1998; Pankhurst et al. 2000; Cawood 2005; Vaughan and Pankhurst 2008; Bahlburg et al. 2009). The Silurian and Devonian mark a hiatus in the magmatic arc record (Chew et al. 2007; Bahlburg et al. 2009), possibly due to changing plate kinematics of the detachment of a segment of the Arequipa-Antofalla block, which is a Precambrian basement block that underlies much of the coastal region of southern Peru (Loewy et al. 2004). Magmatic activity resumed in the Early Mississippian (ca. 345 Ma: Chew et al. 2007; Mišković et al. 2009) and was followed by Late Permian to Late Triassic lithospheric thinning, accompanied by metamorphism and deformation, as well as the emplacement of partially migmatized granitoids at 285–223 Ma (Sempere et al. 2002; Mišković et al. 2009). Easterly subduction of Pacific lithosphere and associated calc-alkaline magmatism in the Western Peruvian Cordillera was re-established by the Late Triassic (Boekhout et al. 2012; Demouy et al. 2012), but was interrupted by a period of back-arc extension and bimodal igneous activity in the Jurassic (Ramos and Aleman 2000; Sempere et al. 2002; Boekhout et al. 2012; Demouy et al. 2012), which is attributed to a global change in plate kinematics (Ramos 2010). The Cretaceous marks the intrusion of the Coastal batholith, a large, linear composite pluton emplaced in the periods 105–101 Ma, 91–82 Ma, and 73–62 Ma (Pitcher et al. 1985; Mukasa 1986; Hildebrand and

Whalen 2014a).

South-central Andes (18–40° S)

The Cordilleran sector defined here as the south-central Andes includes the Andean Range of Bolivia, northern Chile and west-central Argentina from the Arica deflection, at 18° S to 40° S. The basement of the south-central Andes is classically interpreted to be composed by a number of parautochthonous and allochthonous crustal fragments, namely the Pampia, Antofalla, Cuyania, and Chilenia terranes, which accreted to the South American margin at various times throughout the Late Neoproterozoic and Early Paleozoic (Ramos 2009 and references therein). However, based on more recent data, the existence of Pampia, Cuyania (or Precordillera), and Chilenia are contentious (Vaughan and Pankhurst 2008; Alasino et al. 2012; Rapela et al. 2016). Evidence for early magmatic activity in the south-central Andes is found in the Famatinian orogen, a continental magmatic arc active between ca. 505 Ma and 420 Ma (Bahlburg et al. 2009). The Devonian is marked by magmatic and tectonic quiescence along the south-central Andean margin (Bahlburg and Hervé 1997; Chew et al. 2007; Bahlburg et al. 2009; Cardona et al. 2009), but locally, such as in the Sierras Pampeanas in NW Argentina, Middle–Late Devonian A-type granitoids occur (Dahlquist et al. 2013). Continental arc magmatism was widespread during the Late Paleozoic to Early Mesozoic, for example represented by the Chilean Frontal Cordillera Batholith that shows magmatic pulses during the Mississippian, Early Permian, Late Permian–Middle Triassic, and Upper Triassic (Hervé et al. 2014; Maksaev et al. 2014). After another gap in arc magmatic activity during the Late Permian to Late Triassic, subduction was re-established and persisted into the present day in what is referred to as the Andean cycle (Ramos and

Aleman 2000; Haschke et al. 2006). During the Jurassic to Early Cretaceous, extensional tectonics characterized the south-central Andean margin, which led to the development of a magmatic arc located along the present-day coastal Cordillera, and a series of back-arc basins to the east (e.g., Oliveros et al. 2012; Rossel et al. 2013).

Southern Andes (39–55° S)

The southern Andean sector coincides with the tectonic province known as Patagonia, which extends from about 39° S to 55° S. The Paleozoic geological history of Patagonia is not agreed upon in every aspect, but is generally interpreted to have involved the collision of an (para-)autochthonous northern block, and an allochthonous southern block in the Carboniferous (Pankhurst et al. 2006; Ramos 2008; Rapalini et al. 2010; Ramos and Naipauer 2014). Subduction-related magmatic rocks of Early Devonian to Carboniferous age occurring in the North Patagonian Massif are interpreted to reflect the destruction of the ocean basin between these blocks (e.g., Hervé et al. 2013). In the southern block, east-dipping subduction may have commenced at ca. 390 Ma and continued into the Mesozoic (Kato et al. 2008; Chernicoff et al. 2013). Voluminous and regionally extensive Mesozoic to Cenozoic continental magmatic arc activity in the southern Andes is evidenced by the Patagonian batholith that is subdivided into a Late Cretaceous to Late Miocene northern part (Pankhurst et al. 1999), a Late Triassic central part (Rapela and Pankhurst 1992; Zaffarana et al. 2014), and a Late Jurassic to Neogene southern part (Rolando et al. 2002; Hervé et al. 2007).

Methods

Age compilations

Age spectra between 400 and 80 Ma were constructed on the basis of ~1,300 (bulk) U/Pb crystallization ages of igneous bedrocks, and 15,575 detrital zircon U/Pb ages from published and unpublished sources (see appendix for complete list of references). The compilation contains U-Pb analyses only, because Rb/Sr, K/Ar and $^{40}Ar/^{39}Ar$ analyses may yield erroneous ages due to daughter isotope loss, low-grade metamorphism and/or hydrothermal activity post-dating volcanic and plutonic rock emplacement, even in young volcanic rocks (e.g., Montecinos et al. 2008). The age compilation combines TIMS (thermal ionization mass spectrometry), LA-ICP-MS (laser ablation inductively coupled plasma mass spectrometer), SHRIMP (sensitive high-resolution ion microprobe), and SIMS (secondary ion mass spectrometry) analyses. Coordinates were extracted for each bedrock and detrital zircon sample to enable the division of age data into predefined sectors along the Cordilleran arc. To constrain data collection and analyses, we focused on age data between 400 Ma and 80 Ma only. These limits are arbitrary, but were chosen because (i) magmatic arc activity started in the Early Paleozoic in many places along the Cordilleran orogen and terminated at around 80 Ma in the Sierran sector, (ii) the number of available Cenozoic igneous and detrital U/Pb ages is inadequate due to the fact that young igneous arcs are commonly dated with the $^{40}Ar/^{39}Ar$ method and there are less detrital zircon studies of Cenozoic deposits.

Each bedrock age represents a multiple or bulk zircon age of analyses from three or more single zircon grains (or domains therein) that were calculated by the original author. This does not apply for the Sierran sector, for which single zircon bedrock ages have been compiled. The dated rocks summarized as "bedrock ages" comprise chiefly plutonic rocks with a predominantly felsic to intermediate composition and only a few volcanic rocks.

Detrital zircon samples of different depositional age were included in the compilation to sample the maximum number of sources exposed at various times in the geological past. The detrital zircons are interpreted to represent magmatic ages. Zircon ages identified to have a metamorphic origin (mostly based on U/Th ratios) by the original investigators are excluded from the compilation. The concordance of each zircon grain was calculated from $^{206}Pb/^{238}U$ and $^{207}Pb/^{235}U$ ages to ensure that only concordant grains, i.e. with < 10 % normal and < 5 % reverse discordance, were included in the age compilation.

For igneous and detrital zircon data, respectively, age data (Fig. 1) are plotted as (i) histograms with a 10 m.y. bin width, and (ii) kernel density estimates (KDEs; Vermeesch 2012), which are overlain on the histograms. The histograms allow visual evaluation of the number of samples forming age peaks and enable inter-sample comparison, but are constructed using a constant bin size, which may not be appropriate for zircon age distributions, which are neither smooth nor unimodal (e.g., Vermeesch 2012). The calculated KDEs, on the other hand, are based on adaptive kernel density estimation, in which the bandwidth is varied according to the local density. As a smooth and continuous alternative to the discrete and discontinuous histogram, KDEs facilitate the automatic extraction of peaks and other time series parameters and allows normalization and thus the combination of bedrock and detrital zircon age data. KDEs were chosen as a statistical technique to visualize age populations rather than probability density plots

(PDPs) because KDEs are considered statistically more robust than the more commonly used PDP, especially when data quantity and/or precision is high (Vermeesch 2012). Furthermore, because the kernel density estimate does not take into account analytical uncertainties, the different levels of precision of the compiled TIMS, LA-ICP-MS, SHRIMP, and SIMS age data have no effect on the shape of the KDEs. KDE calculation was accomplished using an open-source Java application developed by Peter Vermeesch (Density Plotter, http://www.ucl.ac.uk/~ucfbpve/densityplotter/). Composite KDE functions, in which bedrock and detrital age spectra are combined by summing the respective normalized KDE values for each age interval, are plotted in a space-contour plot (Fig. 2a) to visualize along-arc variation in magmatic activity. Using Gauss fitting, statistical parameters such as peak location, height, prominence, width, and skewness were calculated from these composite KDE functions. Furthermore, a time-series spectral analysis was performed using the Lomb-Scargle method (Lomb 1976; Scargle 1982) to establish whether or not the zircon age spectra exhibit cyclic behavior. The term "cyclic" in this paper is used synonymously with "periodic", and is defined as a repetition of an event or a sequence of events at regular time intervals. The terms "episode" and "episodic", on the other hand, refer to unique or randomly repeated events. The Lomb-Scargle method is based on a fast Fourier transform, in which the individual composite KDE functions (containing both bedrock and detrital zircon ages from each Cordilleran sector) are decomposed into a combination of sinusoids of different frequencies, amplitudes, and phases. Magnitudes in the resulting Lomb-Scargle periodogram (Fig. 2b) represent the contribution of a frequency or period to the original time series. A periodic event or cycle in the data will create a distinct spike in the periodogram. Frequencies or periods with a high spectral magnitude can be attributed to a periodic event, but only if the sampling interval supports at least 3 periods of that frequency (e.g., Telgársky 2013). Hence, only periods up to 100 m.y. are considered.

Geochemical data

In order to investigate how changes in geochemical composition of arc-related igneous rocks correlate with magmatic arc activity, geochemical data are currently being compiled by the authors for all eight arc domains. In this paper, the three datasets from the (i) Sierra Nevada, (ii) Peninsular Ranges, Transverse Ranges, Mojave, and northern Mexico, and (iii) southeastern Mexico and Central America are presented. Flare-up events, identified on composite KDE functions of the individual arc sector by visual gauging of peak distribution, width, and height, were used as a reference for description of trends in geochemical data. The geochemical proxies include SiO_2 to evaluate extent of differentiation, εNd_i and $^{87}Sr/^{86}Sr_i$ to assess the relative roles of crustal and mantle components in arc magmas (e.g., DePaolo and Wasserburg 1979; DePaolo 1981a), and Sr/Y and $(Sm/Yb)_n$ (normalized to chrondrite values) for a measure of magma source depth and crustal thickness (e.g., Gromet and Silver 1987; Mamani et al. 2010; Chapman et al. 2015; Chiaradia 2015; Profeta et al. 2015). Due to the scarcity of available geochemical data with U/Pb zircon ages in the Peninsular Ranges and the southern Mexican sector, U-Pb-zircon constrained data were supplemented by geochemical data with ages constrained by other means in these sectors, including $^{40}Ar/^{39}Ar$, K/Ar, Rb-Sr, and Sm-Nd geochronology, and ages estimated using (bio-)stratigraphic evidence. Apart from the data points, median values ± one standard deviation were plotted for a moving 10 m.y. average to allow a better evaluation of trends and degree of scatter (Fig. 3). In the case of Sr/Y and $(Sm/Yb)_n$, only rocks with < 70 wt.% SiO_2 are plotted to exclude the effect of plagioclase fractionation, affecting Sr/Y, and to exclude garnet bearing granites (e.g., Zhang et al. 2012), affecting both Sr/Y and $(Sm/Yb)_n$.

Kinematic data

In order to investigate the relationship between continental magmatic arc activity and plate kinematics, rates of (i) trench-orthogonal convergence and (ii) trench-parallel displacement between subducting oceanic and upper continental plates, as well as (iii) slab age were compared.

We obtained relative plate motion from a recent plate kinematic model for the interval of 200–0 Ma (Shephard et al. 2013) by using the Python script convergence.py written by Nathaniel Butterworth, EarthByte Group, School of Geosciences, University of Sydney, and based on the pyGPlates application programming interface for GPlates[1] (Boyden et al. 2011). The relative movement of the upper plate was sampled at 24 selected locations (three per arc domain) in the vicinity of the subduction zone vertices in 1 m.y. intervals using GMT[2]. To account for changes in plate motion rate within individual arc domains, these three sets of plate motion values per arc domain were used to calculate and plot average values together with minimum and maximum values (Fig. 3, 4). The slab age, i.e., the age of the plate entering the trench, was extracted for 200–0 Ma in 5 m.y. intervals from paleo-age grids used by Seton et al. (2012) and released in Müller et al. (2013) by applying the same procedure as described above.

To statistically evaluate the link kinematic parameters and magmatic activity, the

[1] http://www.gplates.org/
[2] http://gmt.soest.hawaii.edu/

This is a preprint, the final version is subject to change, of the American Mineralogist (MSA)
Cite as Authors (Year) Title. American Mineralogist, in press.
(DOI will not work until issue is live.) DOI: http://dx.doi.org/10.2138/am-2016-5718

Pearson product moment correlation coefficient, which reflects the extent of a linear relationship, was calculated for each parameter pair after reducing the variables to evenly spaced values (Fig. 5). Age spectra for arc sectors D–H were extended to 50 Ma to allow for a more rigorous evaluation of patterns.

Results

Age compilation

The number of age data for each Cordilleran arc sector varies between a minimum of 112 (SE Mexico and Central America) to a maximum of 257 multiple zircon bedrock ages (Peruvian Andes) or 1678 single zircon bedrock ages (Sierra Nevada), and between 757 (Peruvian Andes) and 5869 (Sierra Nevada) detrital zircon ages. Detrital zircon age spectra are complex, exhibiting many peaks (from 10 in the Sierra Nevada to 29 in the Northern Andes), whereas the igneous spectra are characterized by fewer peaks (from 3 in the Sierra Nevada to 11 in SE Mexico and Central America) of comparatively larger wavelength. KDEs based on bedrock and detrital zircon ages, generally show a similar distribution of peaks, but these peaks may have different relative amplitudes (Fig. 1). In a few cases, maxima in the bedrock age data coincide with minima in the detrital zircon data and vice versa (e.g., at ca. 130 Ma and 275 Ma in F, and at ca. 150 Ma in H), which may be an artifact of relatively low data density in these sectors. The Pearson product moment correlation coefficient, evaluating the similarity between bedrock and detrital age KDE functions, ranges between 0.14 (Peruvian Andes) and 0.87 (Coast Ranges). Correlation coefficients show a bimodal distribution—high values (0.62–0.87) correspond to the North American sectors, whereas the Andean sectors are characterized by low values (0.14–0.42).

The spatial and temporal distribution of maxima and minima of composite KDEs along the Cordilleran arc, displayed in the color contour plot of figure 2a, shows bull's-eye-features reflecting high-amplitude variations of zircon age populations of limited spatial and temporal extent (e.g., ca. 130 Ma minimum in B-C; 134 Ma maximum in D; 200 Ma maximum in E). The figure also shows subtle, along-arc striking linear features of variable length, such as a 105–90 Ma band of high values along A-B-C, a 280–265 Ma band of high values along D-E-F-G-H, and a 175–165 Ma band of high values and 220–210 Ma band of low values along the entire Cordilleran orogen. The Lomb-Scargle periodogram (Fig. 2b) shows relatively high power values at periods of ca. 60–90 m.y. across most of the Cordilleran orogen. In the Coast Ranges, the Peninsular Ranges and the Peruvian Andes, a periodic signal of 80–85 m.y. is particularly pronounced, and periods of ca. 62–68 m.y. have the highest magnitudes in the Sierra Nevada, the South-central and Southern Andes. Smaller, ca. 44–46 m.y. periods are identified in the Coast Ranges, the southeastern Mexican sector and the northern Andes. Other, subordinate, peaks occur at periods of ca. 31 m.y. (Sierra Nevada), 52 m.y. (Peninsular Ranges), 39 m.y. (southeastern Mexico), and 36 m.y. (Northern Andes). Other statistical parameters derived from the composite KDE time series show a high variability, but with increasing age peak height and prominence decreases, and peak width normalized to peak height increases for most of the datasets, as a result of a decrease in analytical precision with increasing age inherent to the geochronological datasets. Peak symmetry also varies within any given arc sector, but is predominantly positively skewed (i.e., has a longer right tail) in the Sierra Nevada, and negatively skewed in the Peninsular Ranges sector.

This is a preprint, the final version is subject to change, of the American Mineralogist (MSA)
Cite as Authors (Year) Title. American Mineralogist, in press.
(DOI will not work until issue is live.) DOI: http://dx.doi.org/10.2138/am-2016-5718

Geochemical data

Sierra Nevada (sector B). For Cordilleran sector B (Fig. 3a), flare-up events (F) occur during the Triassic at ca. 234–213 Ma (F_T), during the Jurassic, at ca. 170–150 Ma (F_J), and during the Cretaceous, at ca. 103–88 Ma (F_C). These flare-up events are separated by periods of low zircon production, i.e. magmatic lulls. Overall, the number of available age-constrained geochemical data in the Sierra Nevada sector is high, ranging between 392 samples (εNd_i) to 3808 samples (SiO_2). The following trends can be observed (Fig. 3a): SiO_2 exhibits higher median values during F_T than during lulls prior and following F_T. From ca. 180 Ma to 90 Ma, median SiO_2 values fluctuate between 60 and 70 wt.%, independent of age relative to a flare-up or lull. SiO_2 increases further from ca. 90 Ma to the end of the observation period. εNd_i exhibits similar median values of ca. -3 during F_T and F_J. Between these two flare-up events, there is a data gap. Subsequent to F_J, εNd_i increases to median values of up to +5, and then decreases back to values around -5 during F_C, and keeps decreasing after F_C. Approximately the inverse trend of that for εNd_i is observed for $^{87}Sr/^{86}Sr_i$, i.e., relatively high values during flare-ups, and low values during lulls. $^{87}Sr/^{86}Sr_i$ data density and scatter are generally lower during lulls than during flare-ups. There is an increase in $^{87}Sr/^{86}Sr_i$ above average values during the last 10 m.y. of the observation period. Sr/Y and $(Sm/Yb)_n$ show almost identical patterns, with highly variable values during flare-ups, but with lower median values than during lulls. At the end of F_C to 80 Ma, both proxies increase to median values above average.

Peninsular Ranges, Transverse Ranges, Mojave, and northern Mexico (sector C).

The number of compiled age-constrained geochemical data in Cordilleran sector D ranges between 221 samples (εNd_i) and 1522 (SiO_2). Flare-up events are recognized within the following approximate limits (Fig. 3b): (F_{PT}) 260–237 Ma, (F_J) 175–160 Ma, (F_{C1}) 110–94 Ma, and (F_{C2}) 86–80 Ma. Median SiO_2 values are lower during F_{PT} and F_J than during periods following these respective flare-up events. From about 120 Ma onwards, SiO_2 fluctuates only slightly around a median value of ca. 67 wt.%. In terms of εNd_i, data density is low for ages up to 180 Ma, but εNd_i seems to decrease from a median of ca. +5 during F_{PT} to a median of ca. -7 in the following lull. Median values form a "plateau" between ages of 180 and 140 Ma. Halfway through the lull between F_J and F_{C1}, εNd_i increases, before decreasing steadily through F_{C1} and F_{C2} until the end of the observation period. There is little $^{87}Sr/^{86}Sr_i$ data for the time up to ca. 130 Ma, but median $^{87}Sr/^{86}Sr_i$ values are relatively high at the end of F_{PT} and shortly prior to F_J. Following F_J, median $^{87}Sr/^{86}Sr_i$ increases from values around 0.705, to about 0.713 halfway through the following lull, before it drops back to 0.705 at the beginning of F_{C1}, and then increases steadily until 80 Ma. Thus, from ca. 130 Ma onward, the $^{87}Sr/^{86}Sr_i$ signal is approximately inverse to the εNd_i signal. Data density is low for Sr/Y in the time prior to 180 Ma. Median Sr/Y values either decrease (F_{PT}, F_J, F_{C2}) or increase (F_{C1}) during flare-up events. Short-lived excursions of median Sr/Y values towards higher values are observed during magmatic lulls. The peak at ca. 220 Ma up to median Sr/Y values of ca. 100 is particularly pronounced. $(Sm/Yb)_n$ shows a similar trend as Sr/Y, with a decrease (F_{PT}, F_J, F_{C2}) or increase (F_{C1}) in median values through flare-up events, and short-lived excursions to higher values during lulls. The peak in $(Sm/Yb)_n$ during F_J is only based on four values. Data scatter is high during F_{C1} and the following lull.

SE Mexico and Central America (sector D). The oldest flare-up event that can be identified in the Cordilleran arc sector D (Fig. 3c) is a Carboniferous, ca. 312–302 Ma event (F_{CA}), which is followed by a Permian, ca. 272–250 Ma event (F_P), a Jurassic, ca. 177–155 Ma event (F_J) and two Cretaceous events at ca. 141–128 Ma (F_{C1}) and 102–94 Ma (F_{C2}), respectively. Within an observation period of 400–80 Ma, the amount of age-constrained geochemical data for southeastern Mexico is only a fraction of that available for sector B and C, i.e., ranges between only 67 samples ($^{87}Sr/^{86}Sr_i$) to 274 samples (SiO_2). Despite overall low data density and occasional data gaps, the following trends are discernable: SiO_2 increases more or less steadily from values around 50 wt.% to values of 70 wt.% that are reached shortly after the end of F_P. The Triassic lull marks a drop in SiO_2 values, before peaking again during F_J. This pattern, of low SiO_2 during lulls, and high SiO_2 during flare-up events, is maintained throughout the next two sets of flare-ups and lulls. During F_{C2}, SiO_2 remains low, but increases towards the end of the observation period. Initial εNd values decrease up to F_P and then oscillate two times between median values of ca. +7 and -2 prior to F_J. Data density is low in the following period, but the lull between F_{C1} and F_{C2} seems to be dominated by high εNd_i, whereas the subsequent flare-up event is accompanied by a decrease in εNd_i values. There is little $^{87}Sr/^{86}Sr_i$ data in the period prior to ca. 230 Ma, but the data suggest that there is an increase in $^{87}Sr/^{86}Sr_i$ values in the period leading up to F_P. During the Triassic lull, $^{87}Sr/^{86}Sr_i$ fluctuates inversely to the εNd_i pattern, reaching extremely high median values at the beginning of F_J. Data is absent during the following lull. The lull between F_{C1} and F_{C2} marks an increase in $^{87}Sr/^{86}Sr_i$ from low to moderately high values. Both Sr/Y and $(Sm/Yb)_n$ patterns are similarly displaying an increase up toward F_P, a fluctuation about low values through most of the Mesozoic (with intermittent data gaps), and finally an increase in the period leading up to F_{C2}.

Kinematic data

Trench-orthogonal convergence rates vary in a non-steady state manner. Rates are predominantly positive for all Cordilleran arc sectors (Fig. 4), i.e., associated with advancing slabs, but small negative values are present during the intervals 200–160 Ma in sector A, 140–130 Ma in sector E, 140–110 Ma in sector F, 98–58 Ma in sector G, and 120–50 Ma in sector H indicating minor episodes of slab retreat. The variation of orthogonal convergence rates within an individual arc sector is usually < 50 mm/a. Higher variation is exhibited by (i) sector A at 160–140 Ma due to the accretion of the Wrangellia Superterrane and associated closure of the Cache Creek Ocean (Shephard et al. 2013), (ii) sector D at 120–110 Ma and 72–65 Ma as a result of changes in the position of the trench leading to a ca. 2000 km offset of the points from the active subduction trench, and (iii) sector E at 200–185 Ma that is due to a combination of the geometry of the subduction zone of the northern Andean sector and highly oblique (sinistral) convergence, leading to positive convergence in the north, and negative convergence in the southern part. The Pearson product moment correlation coefficient (r), providing a statistical means of evaluating the likeness of the composite zircon age spectra and trench-orthogonal plate convergence velocities, shows values between -0.38 (sector D) to 0.62 (sector G) (Fig. 5).

Trench-parallel displacement rates fluctuate between positive (right-lateral) and negative (left-lateral) values in most arc sectors (Fig. 4). Sectors B and C predominantly exhibit right-lateral tectonics throughout the observation period, whereas mainly left-lateral movement is observed in the northern Andean domain. The variation of lateral displacement within an individual arc sector is generally < 80 mm/a. Larger variations are observed in certain intervals due to points getting caught on the other side of trenches as a result of changes in the shape and position of the subduction zones as defined in the plate models. Composite zircon age spectra and trench-parallel displacement rates exhibit r values between -0.24 and 0.52 (Fig. 5).

Slab age data exhibit large wavelength fluctuations that are poorly correlated with the composite KDE age spectra (r = -0.53–0.54). Up to 50 m.y. variations of slab ages within individual arc sectors can be explained by the different temporal resolution of the kinematic data sets (1 m.y. for plate polygon data, 5 m.y. for age grids). Larger variations occur in certain intervals of sectors B, F, and H as a result of two different oceanic plates subducting beneath the same arc domain, i.e. Farallon–Kula in B, Farallon–Phoenix/Chasca in F, and Antarctica–Phoenix in H.

Limits, biases, uncertainties, and artifacts

Age compilations. Preservation bias: The underlying premise of this study is that the observed distributions of U-Pb ages reflect relative changes in the vigor of subduction-related magmatic activity in the Cordilleran arc. However, rather than measuring additions of new crustal material, peaks in zircon age spectra have been argued to reflect times of reduced destruction by subduction erosion (Condie et al. 2009; Hawkesworth et al. 2009; Belousova et al. 2010; Hawkesworth et al. 2010; Condie et al. 2011; Cawood et al. 2012; Hawkesworth et al. 2013). We use a combination of bedrock ages and detrital zircon ages (from samples with different depositional age) to compensate for the fragmentary preservation record of arc magmatism. Hence, although the igneous suite of a certain age may no longer be preserved in situ due to recycling processes occurring at subduction zones, such as subduction erosion (Clift and Vannucchi 2004; Hawkesworth et al. 2009; Scholl and Huene 2009), detrital zircons from sediments in arc-flanking basins may provide a record of the magmatic activity represented by the obliterated crust. Intrinsic factors, such as erodibility and zircon abundance of the source rock, as well as extrinsic factors, such as erosion (climate, relief, etc.) and transport processes (wind and drainage patterns, distance of source to sink, etc.) determine to what degree an igneous source is represented in the detrital zircon record (Cawood et al. 2012). These factors and the issue of preservation likely bias the observed abundance relative to the true abundance in the source area. Hence, the age spectra cannot be used to quantitatively evaluate the mass balance of igneous rocks, but can only be used as a general, qualitative indicator of magmatic arc activity.

Sampling bias: Igneous rocks that are only exposed in remote or logistically challenging areas will be under-represented in the bedrock age spectrum, whereas intense sampling of igneous rocks from small geographic areas can bias the relative significance of a peak in the age spectrum. Furthermore, arc-parallel drainage systems or wind trajectories may potentially introduce zircons from adjacent sectors, yielding extraneous peaks in the detrital zircon spectra of a certain arc domain. Trench-parallel displacements of crustal blocks along strike-slip faults may be another way of introducing external material to any given arc sector. Since the boundaries of the eight arc domains are based on present day geographic location, trench-parallel displacements of crustal fragments, either during or subsequent to the 400–80 Ma observation period, such as those documented in southern California (Luyendyk et al. 1980; Jackson and Molnar 1990; Nicholson et al. 1994), southern Mexico (e.g., Dickinson and Lawton 2001; Elías-Herrera and Ortega-Gutiérrez

This is a preprint, the final version is subject to change, of the American Mineralogist (MSA)
Cite as Authors (Year) Title. American Mineralogist, in press.
(DOI will not work until issue is live.) DOI: http://dx.doi.org/10.2138/am-2016-5718

2002; Pindell et al. 2012), the south-central Andes (Brown 1993; Taylor et al. 1998), and the southern Andes (Cembrano et al. 2002; Rosenau et al. 2006), may distort age spectra of these or adjacent arc domains. Considering that along-arc translations of the mentioned crustal blocks are usually in the range of a few hundred kilometers at the most, and that the geographic limits of individual arc domains mostly coincide with tectonic boundaries, the effects on age spectra imposed by lateral displacements of crustal fragments should be relatively minor.

Tectonic setting bias: Our study is concerned with continental arc magmatism, so we want to compare rocks from the same tectonic setting. The compiled zircon ages, both igneous and detrital, are believed to represent magmatic ages, as zircon ages identified as metamorphic ages by the original investigators, have been excluded. However, apart from being produced in continental arc magmas, igneous zircon can also be generated due to continental collision, or rifting (e.g., Hawkesworth et al. 2009). Collisional processes associated with plate reorganizations during Pangea assembly particularly influence the Northern and Peruvian Andean sectors at 300–230 Ma (Mišković et al. 2009; Spikings et al. 2014), whereas notable episodes of extensional tectonics are documented in sector D at 215–185 (Centeno-García et al. 1993; Martini et al. 2010), in sector E at 240–216 Ma (Spikings et al. 2014), in sector F in the Permo-Triassic (Sempere et al. 2002; Mišković et al. 2009) and Jurassic (Ramos 2010), and in sector G at 200–140 Ma. However, magma volumes generated as a result of continental collision are typically low, and igneous rocks associated with extensional tectonics are predominantly mafic (Storey 1995), and are thus not expected to yield large amounts of zircon (Cawood et al. 2012). Island arcs, which after their formation have collided with the continental margin, potentially represent additional sources of magmatic zircon, and can lead to spurious peaks in the zircon age spectra. Oceanic terranes and island arcs with ages between 400 and 80 Ma are documented in (i) the Coast Ranges, i.e. the Triassic Chelan Mountains terrane (Tabor et al. 1989; Matzel et al. 2008), (ii) the Sierra Nevada, i.e. Early Paleozoic and Jurassic intraoceanic arc complexes in the eastern Klamath and northern Sierra terranes (Colpron and Nelson 2009; Dickinson 2009; Colpron and Nelson 2011) and the Late Paleozoic Golconda Allochthon (Riley et al. 2000), (iii) northern Mexico, i.e. the Early Cretaceous Alisitos arc terrane (Busby 2004), and (iv) southeastern Mexico, i.e. the Middle Jurassic–Lower Cretaceous Guerrero Composite Terrane (Martini et al. 2011; 2013; Palacios-García and Martini 2014). Accumulating evidence indicates that both the Alisitos and the Guerrero Composite Terrane are not far-travelled island arc terranes, but peripheral arc systems that formed due to subduction-related extension at the Mexican continental margin (Busby 2004; Centeno-García et al. 2011 and references therein). In that sense, magmatism relating to these respective terranes is not exotic with respect to the continental arc to which these terranes subsequently accreted, but a result of "accordion" tectonics characteristic of convergent continental margins (e.g., Collins 2002). However, the Alisitos and Guerrero fringing arc terranes are not underlain by continental crust, but by transitional to oceanic crust (Busby 2004; Centeno-García et al. 2011). Hence, compositional data derived from these domains have to be interpreted with care, as there can be a bias towards more juvenile compositions. The contribution of Devonian-aged island arc-derived zircons in the Sierra Nevada arc domain seems to be only minor, as apparent from the age compilation (Fig. 1).

Methodological bias: Plutons in continental arcs are often assembled incrementally (e.g., Barboni et al. 2013; Klemetti and Clynne 2014). The longevity of silicic magmatic systems can lead to complex growth of zircon, which may impart a positive age bias. Furthermore, age analyses acquired by techniques in which zircons are not treated by chemical abrasion may be affected by lead loss (e.g., Crowley et al. 2015; Schaltegger et al. 2015), possibly imparting a negative age bias. For the compilation of bedrock ages, which are multi-zircon ages (except for Sierra Nevada bedrock ages) we blindly accept the interpretation of the original authors that these represent the true crystallization age of the igneous rock. For detrital zircon data, the statistical adequacy, i.e., to what degree the observed age abundance matches the corresponding abundance in the sediment, is influenced by the number of grains analyzed and by the sample preparation procedure. An artificial bias introduced during sample preparation and an insufficient number of zircon grains analyzed per sample may cause certain age populations to go undetected, or result in spurious peaks in the age spectra (e.g., Dodson et al. 1988; Sircombe 2000; Vermeesch 2004; Andersen 2005). As with the bedrock data, we have compiled detrital zircon data with no regard for the statistical robustness of the individual datasets, thus accepting the methodological choices made by the original investigators. An additional factor that may influence the distribution of peaks in the age spectra concerns the representation of age frequency data. For histograms of this study, a constant bin size of 10 Ma, which corresponds to the average value of "ideal" bin widths as calculated for every dataset using Sturge’s or Rice’s rule, was chosen to allow a comparison between datasets. However, because zircon age distributions are neither smooth nor unimodal, choosing a constant band- or bin-width to visualize age frequency data may not be

This is a preprint, the final version is subject to change, of the American Mineralogist (MSA)
Cite as Authors (Year) Title. American Mineralogist, in press.
(DOI will not work until issue is live.) DOI: http://dx.doi.org/10.2138/am-2016-5718

appropriate (e.g., Vermeesch 2012). Hence, in addition to histograms, kernel density estimates (KDEs) are used for statistical analyses of the age data. For the calculation of KDEs, bandwidths are varied according to local density, i.e., where data density is low, a large bandwidth is used resulting in a smoothed distribution, and in parts with abundant data, a narrower bandwidth is used providing a higher resolution (Vermeesch 2012). The resulting KDEs of the detrital zircon datasets, each based on 757 data points and more, locally exhibit frequency variations on the order of ca. 3–5 Ma, whereas generally low data density in bedrock data results in relatively large-scale temporal variations in the KDE at a resolution of ca. 20–40 Ma. Hence, the temporal resolution of bedrock data only allows the identification of large-scale temporal variations in arc-magmatism.

Geochemical data. Preservation bias: Geochemical data may be biased by the ages of the material preserved and sampled, so they underlie the same biases and uncertainties that apply for the age compilations.

Sampling bias: The Alisitos and Guerrero fringing arc terranes of Triassic to Jurassic age, which cover a substantial area in arc domains C and D, respectively, are not underlain by continental crust, but by transitional to oceanic crust (Busby 2004; Centeno-García et al. 2011), which causes a bias towards more juvenile compositions in this age interval. Hence, caution should be used in interpretations concerning crustal vs. mantle components in arc magmas as well as estimates of crustal thickness. Slab window formation, slab tearing or cracking, and slab detachment may cause upwelling of hotter asthenospheric mantle and associated adakite-type igneous activity in certain arc segments (e.g., Yogodzinski et al. 2001). Compositional data may furthermore be affected by inboard or outboard migration of the continental arc due to changes in the angle of the subducting slab, episodes of subduction erosion, or accretion of terranes. Spatial migration of the arc may shift the focus of magmatism to areas where the crust exhibits differing thermal or compositional properties, potentially introducing artifacts into the compositional data. The location of continental arcs may be traced by the distribution of currently exposed igneous rocks, and to a lesser degree by the distribution of detrital zircon populations. In southeastern Mexico and Central America, for example, the Carboniferous–Permian arc seems to spatially coincide with the Jurassic (Nazas) arc, whereas the Cretaceous arc is located further outboard, due to the accretion of the Guerrero Composite Terrane in the Early Cretaceous (Fig. 6).

Tectonic setting bias: In this paper, we intend to compare the compositions of igneous rocks that are a product of continental arc magmatism only. Whereas excluding data associated with other tectonic settings is difficult for zircon age data, compositional data can be filtered using suitable proxies and threshold values. For instance, according to Pearce et al. (1984), Yb+Ta values allow an effective separation of igneous rocks of volcanic arcs (Yb+Ta < 6) from those of within plate settings and ocean ridges (Yb+Ta > 6). However, applying this constraint to major element and isotopic data results in a reduction in the number of samples by up to 80 % (e.g., SiO_2 values in the Sierra Nevada sector), caused not by a within-plate signature of the samples, but predominantly due to the fact that major element and isotopic data are rarely accompanied by Yb and Ta values. Overall, the Yb+Ta filter yields negligible changes in the general pattern of the compositional data. Hence, in figure 3, the complete and unfiltered datasets are presented.

Methodological bias: Mafic rocks are notoriously difficult to date by U-Pb zircon methods, hence, mafic rocks may be underrepresented in the geochemical dataset. However, U-Pb-zircon constrained data were supplemented by geochemical data with ages constrained by other means, including $^{40}Ar/^{39}Ar$, K/Ar, Rb-Sr, and Sm-Nd geochronology, and ages estimated using (bio-)stratigraphic evidence. These dating techniques should not be greatly affected by magma chemistry. A problem with $^{40}Ar/^{39}Ar$, K/Ar, Rb-Sr, and Sm-Nd geochronology, however, is an increased risk of daughter isotope loss brought about by low-grade metamorphism and/or hydrothermal activity post-dating volcanic and plutonic rock emplacement. This may result in erroneous ages, i.e. affect the position of data points along the x(time)-axis, and in the case of Nd and Sr isotopic data, also along the y-axis, as ages are used to calculate the initial Nd and Sr compositions. Plotting median values ± one standard deviation for a moving 10 m.y. average allows for a fast evaluation of trends and degree of scatter. However, the median and standard deviation of the compositional data are strongly influenced by the size of bins. A bin size of 10 m.y. has been chosen for all geochemical proxies of this study (independent of sample size, to allow comparison between datasets), as this seems appropriate for an analysis on this temporal scale, but this precludes the recognition of smaller-scale compositional variations.

Uncertainties concerning magma source: Continental arc magmas reflect variable contributions from mantle, crustal and subducted reservoirs (e.g., Hildreth and Moorbath 1988; Hawkesworth et al. 1993; Jones et al. 2015). In this paper the geochemical proxies Sr/Y and Sm/Yb are in this paper primarily used to estimate magma source depth and crustal thickness (e.g., Mamani et al. 2010; Chapman et al. 2015; Chiaradia 2015; Profeta et al. 2015). Magmas of thicker arcs evolve at deeper average levels, stabilizing amphibole ± garnet at the expense of plagioclase in the mineral assemblage of residual magmas and partial melts (e.g., Kay 1978; Defant and Drummond 1990; Mahlburg Kay and Mpodozis 2001). Given the marked affinity of Yb for garnet, Y for garnet and amphibole, and Sr for plagioclase, higher Sr/Y and Sm/Yb values arguably indicate amphibole and garnet-dominated melts sources (either lower crustal residue or deep mantle), and thus, a thicker crust. However, there are several additional processes that can have an impact on the Sr/Y ratio, such as (i) a contribution of slab melts (e.g., Defant and Kepezhinskas 2001; König et al. 2006; Chiaradia 2015), (ii) plagioclase fractionation, and (iii) crustal anatexis producing garnet-bearing granites (e.g., Zhang et al. 2012). While adakitic rocks derived from slab melts are relatively rare in continental arcs, only rocks with < 70 wt.% SiO_2 are plotted for Sr/Y and $(Sm/Yb)_n$ to exclude the effect of plagioclase fractionation, and to exclude highly felsic garnet-bearing granites.

Kinematic data. Our analysis implicitly accepts the respective plate motion models and the geodynamic concepts upon which these are based. However, due to the progressive destruction of oceanic lithosphere by subduction, uncertainties associated with paleogeographic reconstructions increase with age. For example, the link between South America and the subducting Farallon Plate must be determined indirectly by a series of intermediate rotations, called plate circuits, because subduction has consumed most of Panthalassa's oceanic plates (e.g., Seton et al. 2012). The Farallon-South America plate circuit involves five "hops" via the Farallon, Pacific, West and East Antarctic, African, and finally, South American Plates. The link through the Pacific Plate is only possible for times since the Late Cretaceous, when seafloor spreading between the Pacific and West

Antarctic Plates was established (e.g., Eagles et al. 2004; Wobbe et al. 2012). For the time prior to the Late Cretaceous, a hotspot reference system must be used for the Pacific Plate (Seton et al. 2012). The Early Cretaceous separation of Patagonia from Africa involved substantial intracontinental extension, which led to misfits in the South Atlantic plate reconstruction. Several models have been proposed to minimize uncertainties in the block rotation between Patagonia and South America (e.g., Eagles 2007; Torsvik et al. 2009; Heine et al. 2013), but they show large discrepancies. Similar problems exist for other portions of the Cordilleran margin. Plate kinematic parameters used in this paper must thus be considered with care and applied to first-order processes only.

Discussion

Testing of models

There are two schools of thought on what governs the episodic behavior of arc systems. One set of models invokes events outside the arc, such as plate reconfigurations and changes in mantle flow and/or magma production as the ultimate driver of magmatic activity in arcs (e.g., Armstrong 1988; Hughes and Mahood 2008; Zellmer 2008; de Silva et al. 2015), whereas another set of models is based on arc-internal feedback processes involving magmatic/tectonic crustal thickening, crustal melting, and delamination (Karlstrom et al. 1993; Ducea 2001; DeCelles et al. 2009; Karlstrom et al. 2014; Chin et al. 2015; DeCelles et al. 2015; Cao et al. 2016). These sets of models predict differences in terms of the spatial distribution and the temporal scale of magmatic activity as well as the relationship between magmatic activity and magma composition, and kinematic parameters, respectively. More specifically, if arc systems were externally controlled, i.e.

governed by parameters of the down-going plate, such as convergence rate, age, and subduction angle, flare-ups and lulls in magmatic activity would likely be widely distributed along the arc and occur as distinct (random) events that may coincide with periods of global plate reorganization. In contrast, models invoking an internal forcing should be independent of plate parameters, and are often characterized by cyclic behavior, i.e. events recurring at regular intervals. Flare-ups and lulls would also be spatially limited, because, depending on the crustal architecture of the arc sector, different parts may be at different stages in the cycle at any given time. Furthermore, arc-internal processes, such as crustal thickening, delamination, etc., predict changes in arc chemistry that should correspond to variations in magmatic activity, whereas no such correlation is expected in the case of an external forcing. These criteria are discussed in the following sections.

Spatial and temporal pattern. The distribution of U/Pb bedrock and detrital zircon ages, used as a proxy for the timing of magmatic accretion, shows a great variability in the spatial scales of Cordilleran magmatic arc activity (Fig. 2). Some minima and maxima are nearly synchronous for thousands of km along the arc. Other peaks and troughs, although the period may be the same, are “shifted” by up to 30 m.y. from one sector to the next (e.g. Permo-Triassic flare-up and lull in sector B and C). On one hand, these features suggest an external, i.e. plate tectonic influence on Cordilleran arc magmatism; on the other, they highlight the importance of internal feedback processes operating independently in different sectors due to distinct crustal properties.

Previous studies in Cordilleran magmatic arcs suggest that flare-up events occur with a periodicity of 25–45 m.y. in the Central Andes (Haschke et al. 2006), and 20–50 m.y. in different parts of the North American Cordilleras (Barton 1996; Ducea 2001; Gehrels et al. 2009; Mahoney et al. 2009; Paterson et al. 2011; Barth et al. 2013; DeCelles et al. 2015). Our analysis shows that while periods between 20 and 50 m.y. are present in the dataset, a period of ca. 60 to 80 m.y. is more prominent in the Cordilleran orogen, although the relative magnitude of this periodicity is highly variable for different sectors. In models advocating internal feedback processes in the upper plate as a control of arc magmatism, the periodicity signal is often attributed to a cyclic development and subsequent removal of a crustal arc root (e.g., Ducea 2001; DeCelles et al. 2009; Karlstrom et al. 2014; Chin et al. 2015; DeCelles et al. 2015). According to a recent numerical model (Lee and Anderson 2015), which does not factor in tectonics or erosion, these processes have a period of 10–30 million years. The presence or absence of a periodic component in itself may be diagnostic of either an internal or an external control on arc magmatism, respectively. Although supercontinent formation, too, has been suggested to be cyclic (Nance et al. 2014 and references therein), it exhibits a period of 250–320 m.y. and hence it is not directly apparent in the lifetime of Cordilleran arcs. However, processes associated with the fragmentation and assembly of supercontinents may register as distinct events in the record of magmatic activity that may be superimposed on any cyclicity, or even cause cycles to become interrupted or (re-) initiated. The observed variability in period and magnitude are likely a consequence of a superposition of different processes, both cyclic and random.

Relationship with magma chemistry. Annen et al. (2006) state that although melt production in the lower crust strongly depends on emplacement rate of mantle-derived basalt, crustal melting is limited by the availability of fertile crust that can be partially melted. In the model by DeCelles et al. (2009; 2015) the availability of fertile crustal material is the driving force of magmatic episodicity. According to this model, periods of high arc magma production in the continental arc are fueled by underthrusting of forearc and/or retroarc lithosphere, which may also be brought about by slab shallowing (Chapman et al. 2013) or increased plate convergence (DeCelles et al. 2015). Hence, the correlation between convergence rates and continental arc magmatism apparent in our data can also be interpreted to reflect a relationship between convergence rates and the rate at which melt-fertile continental lithosphere is fed into the zone of high heat flux and melting (DeCelles et al. 2015). In terms of arc magma geochemistry, this crustal thickening model predicts SiO_2, $^{87}Sr/^{86}Sr_i$, Sr/Y, $(Sm/Yb)_n$ to be proportional, and εNd_i inversely proportional to arc magma production (DeCelles et al. 2009). The presented geochemical data in this paper generally shows a good correlation between geochemistry and arc magma production, but with notable limitations: (i) In the Sierra Nevada, the expected increase in $^{87}Sr/^{86}Sr_i$, Sr/Y, $(Sm/Yb)_n$ during flare-ups is not as pronounced for the Triassic and Jurassic flare-up event as for the Cretaceous event. Accordingly, numerical modeling (Cao et al. 2016) suggests that crustal thickening was not as pronounced for the pre-Cretaceous flare-up events. Furthermore, the Early Cretaceous marks a period of high variation in Sr/Y and $(Sm/Yb)_n$ ratios that finds no expression in the age spectrum. (ii) The Peninsular Ranges and northern Mexico sector shows an anti-correlation between SiO_2 and zircon age density estimates for the time prior to ca. 130 Ma. Moreover, there are short periods of elevated Sr/Y and $(Sm/Yb)_n$ ratios during magmatic lulls. (iii) Southeastern Mexico and Central America exhibit relatively low SiO_2, high εNd_i, and low $(Sm/Yb)_n$ during the Carboniferous flare-up event. In addition, the Triassic lull is characterized by low εNd_i and high $^{87}Sr/^{86}Sr_i$.

These observations suggest that not every flare-up event is associated with thick crust, and not every lull is associated with thin crust, so other factors apart from a periodic modulation of crustal thickness may be important in governing the rates of magma production in continental arcs. Even if age and geochemical patterns show the correlation predicted by crustal thickening and ensuing delamination of arc roots, these mechanisms may not be the only explanation. Instead, an increase in SiO_2, $^{87}Sr/^{86}Sr_i$, Sr/Y, $(Sm/Yb)_n$, and a decrease in εNd_i may reflect a migration of the arc through crust with different properties. In the Peninsular Ranges Batholith, where the Cretaceous flare-up event is marked by a west–east progression from an oceanic arc to a continental arc setting (e.g., Morton et al. 2014), overall chemical changes within this corridor (Fig. 3b) are likely the result of an associated increased proportion of assimilated continental material. Hence, the flare-up event may not have been triggered by crustal thickening, but by an increase in mantle input (Paterson et al. 2016).

Relationship with plate parameters. The source region for arc magmas is located in the mantle beneath the arc, where melts are generated as a result of fluid release from the subducted slab (e.g., Gill 1981; Arculus 1994; Tatsumi and Eggins 1995) and mantle decompression caused by subduction-induced corner-flow (e.g., Elkins Tanton et al. 2001; England and Katz 2010). Next to lithospheric thickness of the overriding plate, which may determine the length of the melting column in the mantle wedge (e.g., England et al. 2004; Karlstrom et al. 2014; Chin et al. 2015), subduction parameters such as convergence rate or slab age have also been proposed to influence the wedge thermal structure and extent of melting beneath arcs (Peacock 1990; Iwamori 1998; Hebert et al.

2009; England and Katz 2010; Turner and Langmuir 2015a; 2015b). Higher convergence rates have been shown to (i) lead to more vigorous hydration of the mantle wedge causing increased melting (e.g., Cagnioncle et al. 2007; Plank et al. 2009) and/or (ii) increase the flux of hot mantle into the wedge corner, raising the temperature and causing increased melt formation beneath the arc (England and Wilkins 2004; England and Katz 2010; Turner and Langmuir 2015a; 2015b). In terms of the age of the ocean floor, two competing processes may invoke magma formation in the mantle: fluid fluxing (proportional to age; e.g., Leeman 1996; Hebert et al. 2009) and thermal gradient (inversely proportional with age; e.g., England et al. 2004).

Igneous rocks with mafic–ultramafic composition that are in equilibrium with the mantle wedge are scarce in exposed portions of continental arcs due to density filtering and internal modification processes of ascending magmas in the continental crust, mainly by a combination of fractional crystallization of primary magmas, and partial melting and/or assimilation of crustal material (DePaolo 1981b; Hildreth and Moorbath 1988; Tatsumi and Stern 2006). The majority of models for the generation of intermediate melts characteristic of continental arcs invokes processes occurring at lower crustal depth, such as underplating, or the intrusion of mafic magma in the form of sills and/or dykes (Huppert and Sparks 1988; Bergantz 1989; Petford and Gallagher 2001; Annen and Sparks 2002; Jackson et al. 2003; Annen et al. 2006; Otamendi et al. 2009; Jagoutz 2010; Otamendi et al. 2012). The extent to which magma production in the mantle influences the rate at which magmas migrate to upper crustal levels is an issue of much controversy (e.g., de Silva et al. 2015). Numerical models show that, to a first order, a higher basalt emplacement rate into the lower crust leads to an increase in the production of residual

(DOI will not work until issue is live.) DOI: http://dx.doi.org/10.2138/am-2016-5718

melts (due to crystallization of basalt) and partial melts (Bergantz 1989; Barboza et al. 1999; Barboza and Bergantz 2000; Dufek and Bergantz 2005; Annen et al. 2006), although it is known that magma transfer rates through the crust are also dependent on other second order factors, such as the initial geotherm as well as crustal thickness, stress state, density, and composition (e.g., Lima et al. 2012; Chaussard and Amelung 2014).

If convergence rates and plate ages governed melt production in the mantle wedge, and if the magma transferred to the middle and upper crust was proportional to the magma advected from the mantle wedge (e.g., Zellmer and Annen 2008), there should be a correlation between plate parameters and magmatic arc activity. Although some studies (e.g., Armstrong 1988; Hughes and Mahood 2008; Zellmer 2008) provide evidence of such a correlation, others (e.g., Ducea 2001; DeCelles et al. 2009; 2015; Cao et al. 2016) have negated such a link, because flare-up events in some parts of the Cordillera are seemingly out of sync with peaks in convergence rates. However, the latter studies are based on spatially and temporally limited geochronological and plate motion data (e.g., Engebretson et al. 1985; Pardo Casas and Molnar 1987; Somoza 1998; Sdrolias and Müller 2006). Our compilation of geochronological data and plate parameters extracted from a modern global plate motion model (Seton et al. 2012) that extends back to 200 Ma allows us to re-evaluate the strength of this relationship on a broader scale. The data show that the degree of correlation between orthogonal convergence rates and age spectra is generally poor, but highly variable from one Cordilleran arc sector to the next. However, if variable lag times (up to 10 m.y.) are introduced to account for an incubation period or thermal lag as the system adapts to a new configuration between magmatic episodes (e.g., Annen et al. 2006; de Silva et al. 2006; Mamani et al. 2010; Paterson and Ducea 2015), it leads to a notable increase (up to 2.0 times) in the correlation coefficient for several sectors, resulting in a moderate ($0.3 < r < 0.5$) to high ($0.5 < r < 1.0$) degree of correlation for all sectors but the southeastern Mexican (Fig. 7). For pre-Jurassic times, no plate parameters can be extracted due to the lack of a reliable plate model, but certain maxima and minima in the along-arc age correlation chart (Fig. 2) coincide with known tectonic events along the Pacific margin of Pangea, such as (i) the onset of the Pan-Pacific Gondwanide Orogeny at ca. 300 Ma (e.g., Cawood 2005; Cawood and Buchan 2007), (ii) the closure of the Panthalassan Gondwana suture at ca. 250 Ma (Scotese 1997; Cocks and Torsvik 2002; Stampfli and Borel 2002; Murphy and Nance 2008), and (iii) the opening of the central Atlantic and dispersal of Gondwana at ca. 200 Ma (Nance et al. 2012; Seton et al. 2012; Keppie 2015). These events are associated with global plate kinematic reorganization, affecting the direction and speed of plate convergence along the Cordilleran orogen. A major plate reorganization event also occurred at ca. 100 Ma (Matthews et al. 2012), which may have triggered the Cretaceous flare-up events in the Northern Cordilleran sectors (Fig. 2). Together, these data suggest that a possible link between arc-external events and magmatic episodicity should be re-evaluated and once again explored as larger and more precise geochronological and plate kinematic datasets become available.

Future research

The geochronological, geochemical, and plate kinematic database that form the foundation of this study are a work in progress. Increasing the sample size as more data become available, adding more geochemical/isotopic proxies, and amplifying the temporal and spatial range will allow more rigorous interpretations of these large datasets in terms of characterizing episodic arc magmatism and testing model predictions. To minimize the sampling bias, time dependent magma addition rates need to be determined from retro-deformed surface areas of magmatic rocks and geobarometric data (Matzel et al. 2006; Paterson et al. 2011; Memeti et al. 2014; Paterson and Ducea 2015). Lithospheric stress state is a crucial parameter in models of arc magmatism (e.g., DeCelles et al. 2009; 2015) and a controlling factor for magma ascent; hence establishing structural databases is essential in order to estimate rates of tectonic shortening. Another critical aspect concerns the temporal record of island arc magmatism. Lacking the density filter of thick continental crust, oceanic arcs can provide a simpler, more direct way of studying cause and effect, so obtaining large temporal records for island arcs would be desirable. However, this is a difficult task, because island arcs are often short-lived, usually poorly preserved, and predominantly mafic, the latter of which makes them harder to date by zircon geochronology. Preliminary age records from the Talkeetna, Aleutian, and Kohistan island arcs (Paterson and Ducea 2015), however, show a certain degree of episodicity, suggesting that plate parameters and the availability of mantle melts play a big part in governing arc magmatism, irrespective of the thickness and composition of the upper plate. Oceanic arcs can also be used to estimate the background magma production rate of continental arcs. Recent studies have shown that magma production rates in intraoceanic arcs are comparable to the volumes of magma produced during flare-ups in continental arcs (Jicha and Jagoutz 2015). This means that instead of finding a process to explain increased magma production during flare-ups, a mechanism is needed to temporarily suppress magma production in continental arcs, such as flat slab subduction (e.g., McGeary et al. 1985; Gutscher et al. 2000; Stern 2004).

Implications

We examine large geochronological, geochemical and kinematic data sets for the Cordilleran orogen as a means to test existing models for episodic magmatism in continental arcs. Bedrock and detrital U-Pb zircon age distributions, which have been shown to be qualitative indicators of magmatic activity within the arc, show a clear non-steady state pattern of variable temporal and spatial scales. Whereas most flare-up events are discrete in time and space, some are synchronous for many thousand kilometers along arc-strike, and a moderate periodicity between 60 and 80 million years is apparent in certain portions of the Cordilleran orogen. Covariations between arc magma chemistry and magmatic arc activity suggest crustal thickening during flare-up events, but arc migration poses a challenge, as it can produce similar geochemical patterns. Kinematic data based on recent global plate reconstructions provide a means of evaluating mantle heat input. The correlation between orthogonal convergence rate and Cordilleran arc activity as well as the coincidence between certain flare-up events and lulls with global events of plate tectonic reorganization demonstrates that an external control of continental arc magmatism should be reevaluated. Our results suggest that the driving mechanisms for flare- ups/lulls vary along this Mesozoic arc and that second order effects vary between flare-ups and arc segments.

Acknowledgements

We thank George Bergantz and Alan Chapman for their constructive reviews, and David London for his role as Associate Editor. Kirsch is grateful to Nathaniel Butterworth for the convergence python script and to Maria Helbig and Uwe Kroner for helpful discussions. Paterson acknowledges support from NSF grants EAR-1019636, EAR-0537892 and EAR-0073943 and USGS EDMAP grants G13AC00120 and 03HQA0038. We thank Mark Pecha, and other lab

scientists from the Arizona LaserChron Center for help while using their geochronology lab.

References

Alasino, P.H., Dahlquist, J.A., Pankhurst, R.J., Galindo, C., Casquet, C., Rapela, C.W., Larrovere, M.A., and Fanning, C.M. (2012) Early Carboniferous sub- to mid-alkaline magmatism in the Eastern Sierras Pampeanas, NW Argentina: A record of crustal growth by the incorporation of mantle-derived material in an extensional setting. Gondwana Research, 22, 992–1008.

Andersen, T. (2005) Detrital zircons as tracers of sedimentary provenance: limiting conditions from statistics and numerical simulation. Chemical Geology, 216, 249–270.

Annen, C., and Sparks, R.S.J. (2002) Effects of repetitive emplacement of basaltic intrusions on thermal evolution and melt generation in the crust. Earth and Planetary Science Letters, 203, 937–955.

Annen, C., Blundy, J.D., and Sparks, R.S.J. (2006) The genesis of intermediate and silicic magmas in deep crustal hot zones. Journal of Petrology, 47, 505–539.

Arculus, R.J. (1994) Aspects of magma genesis in arcs. Lithos, 33, 189–208.

Armstrong, R.L. (1974) Magmatism, orogenic timing, and orogenic diachronism in the Cordillera from Mexico to Canada. Nature, 247, 348–351.

Armstrong, R.L. (1988) Mesozoic and early Cenozoic magmatic evolution of the Canadian Cordillera. In S.P. Clark Jr., B.C. Burchfiel, and J. Suppe, Eds., Processes in continental lithospheric deformation. Geological Society of America Special Paper 218, pp. 55–92.

Bahlburg, H., and Hervé, F. (1997) Geodynamic evolution and tectonostratigraphic terranes of northwestern Argentina and northern Chile. Geological Society of America Bulletin, 109, 869–884.

Bahlburg, H., Vervoort, J.D., Frane, Du, S.A., Bock, B., Augustsson, C., and Reimann, C. (2009) Timing of crust formation and recycling in accretionary orogens: Insights learned from the western margin of South America. Earth-Science Reviews, 97, 215–241.

Barboni, M., Schoene, B., Ovtcharova, M., Bussy, F., Schaltegger, U., and Gerdes, A. (2013) Timing of incremental pluton construction and magmatic activity in a back-arc setting revealed by ID-TIMS U/Pb and Hf isotopes on complex zircon grains. Chemical Geology, 342, 1–18.

Barboza, S.A., and Bergantz, G.W. (2000) Metamorphism and anatexis in the Mafic Complex contact aureole, Ivrea Zone, northern Italy. Journal of Petrology, 41, 1307–

1327.

Barboza, S.A., Bergantz, G.W., and Brown, M. (1999) Regional granulite facies metamorphism in the Ivrea zone: Is the Mafic Complex the smoking gun or a red herring? Geology, 27, 447–450.

Barboza-Gudiño, J.R., Hoppe, M., Gómez-Anguiano, M., and Martínez-Macías, P.R. (2004) Aportaciones para la interpretación estratigráfica y estructural de la porción noroccidental de la Sierra de Catorce, San Luis Potosí, México. Revista Mexicana de Ciencias Geológicas, 21, 299–319.

Barboza-Gudiño, J.R., Orozco-Esquivel, M.T., Gómez-Anguiano, M., and Zavala-Monsiváis, A. (2008) The Early Mesozoic volcanic arc of western North America in northeastern Mexico. Journal of South American Earth Sciences, 25, 49–63.

Barth, A.P., and Wooden, J.L. (2006) Timing of magmatism following initial convergence at a passive margin, southwestern U.S. Cordillera, and ages of lower crustal magma sources. Journal of Geology, 114, 231–245.

Barth, A.P., Tosdal, R.M., Wooden, J.L., and Howard, K.A. (1997) Triassic plutonism in Southern California; southward younging of arc initiation along a truncated continental margin. Tectonics, 6, 290–304.

Barth, A.P., Wooden, J.L., Howard, K.A., and Richards, J.L. (2008) Late Jurassic plutonism in the southwest U.S. Cordillera. In J.E. Wright and J.W. Shervais, Eds., Ophiolites, Arcs, and Batholiths A Tribute to Cliff Hopson. Geological Society of America Special Paper 438, pp. 379–396.

Barth, A.P., Wooden, J.L., Jacobson, C.E., and Economos, R.C. (2013) Detrital zircon as a proxy for tracking the magmatic arc system: The California arc example. Geology, 41, 223–226.

Barton, M.D., Battles, D.A., Debout, C.E., Capo, R.C., Christensen, J.N., Davis, S.R., Hanson, R.B., Michelson, C.J., and Trim, H.G. (1988) Mesozoic contact metamorphism in the western United States. In W.G. Ernst, Ed., Metamorphism and Crustal Evolution of the Western United States, Rubey Volume 7: Englewood Cliffs, New Jersey, Prentice Hall, p. 110–178.

Barton, M.D. (1996) Granitic magmatism and metallogeny of southwestern North America. Earth and Environmental Science Transactions of the Royal Society of Edinburgh, 87, 261–280.

Bateman, P.C. (1992) Plutonism in the central part of the Sierra Nevada batholith, California, 572 p., Boulder, Colorado.

Belousova, E.A., Kostitsyn, Y.A., Griffin, W.L., and Begg, G.C. (2010) The growth of the continental crust: constraints from zircon Hf-isotope data. Lithos, 119, 457–466.

Bergantz, G.W. (1989) Underplating and Partial Melting: Implications for Melt Generation and Extraction. Science, 245, 1093–1095.

Boekhout, F., Spikings, R., Sempere, T., Chiaradia, M., Ulianov, A., and Schaltegger, U. (2012) Mesozoic arc magmatism along the southern Peruvian margin during Gondwana breakup and dispersal. Lithos, 146-147, 48–64.

Bouysse, P., Heyd, C., and Rambourg, D. (2010) Geological map of the world at 1:50,000,000 (3rd ed.), 2 sheets. Commission for the Geological Map of the World, UNESCO, Paris.

Boyden, J.A., Müller, R.D., Gurnis, M., Torsvik, T.H., Clark, J.A., Turner, M., Ivey-Law, H., Watson, R.J., and Cannon, J.S. (2011) Next-generation plate-tectonic reconstructions using GPlates. In Geoinformatics: Cyberinfrastructure for the Solid Earth Sciences pp. 95–114. Cambridge University Press, Cambridge.

Bradley, D.C. (2008) Passive margins through earth history. Earth-Science Reviews, 91, 1–26.

Brown, M. (1993) Displacement history of the Atacama fault system 25°00′S- 27°00′S, northern Chile. Geological Society of America Bulletin, 105, 1165–1174.

Burchfiel, B.C., and Davis, G.A. (1972) Structural framework and evolution of the southern part of the Cordilleran orogen, western United States. American Journal of Science, 272, 97–118.

Burchfiel, B.C., and Davis, G.A. (1975) Nature and controls of Cordilleran orogenesis, western United States: Extensions of an earlier synthesis. American Journal of Science, 275A, 363–396.

Busby, C. (2004) Continental growth at convergent margins facing large ocean basins: a case study from Mesozoic convergent-margin basins of Baja California, Mexico. Tectonophysics, 392, 241–277.

Bustamante, C., Cardona, A., Bayona, G., Mora, A., Valencia, V., Gehrels, G., and Vervoort, J. (2010) U-Pb LA-ICP-MS geochronology and regional correlation of Middle Jurassic intrusive rocks from the Garzon Massif, Upper Magdalena Valley and Central Cordillera, southern Colombia. Boletín de Geología, 32, 1–17.

Cagnioncle, A.-M., Parmentier, E.M., and Elkins-Tanton, L.T. (2007) Effect of solid flow above a subducting slab on water distribution and melting at convergent plate boundaries. Journal of Geophysical Research, 112, B09402.

Campa, M.F., and Coney, P.J. (1983) Tectono-stratigraphic terranes and mineral resource distributions in Mexico. Canadian Journal of Earth Sciences, 20, 1040–1051.

Campa-Uranda, M.F., García Díaz, J.L., and Iriondo, A. (2004) El arco sedimentario del Jurásico Medio (Grupo Tecocoyunca y Las Lluvias) de Olinalá. GEOS Unión

Geofísica Mexicana, 24, 174.

Cao, W., Paterson, S., Saleeby, J., and Zalunardo, S. (2016) Bulk arc strain, crustal thickening, magma emplacement, and mass balances in the Mesozoic Sierra Nevada arc. Journal of Structural Geology, 84, 14–30.

Cardona, A., Cordani, U.G., Ruiz, J., Valencia, V.A., Armstrong, R., Chew, D., Nutman, A., and Sanchez, A.W. (2009) U-Pb zircon geochronology and Nd isotopic signatures of the pre-Mesozoic metamorphic basement of the eastern Peruvian Andes: growth and provenance of a Late Neoproterozoic to Carboniferous accretionary orogen on the northwest margin of Gondwana. The Journal of Geology, 117, 285–305.

Cardona, A., Valencia, V., Garzón, A., Montes, C., Ojeda, G., Ruiz, J., and Weber, M. (2010) Permian to Triassic I to S-type magmatic switch in the northeast Sierra Nevada de Santa Marta and adjacent regions, Colombian Caribbean: Tectonic setting and implications within Pangea paleogeography. Journal of South American Earth Sciences, 29, 772–783.

Carmona, O.O., and Pimentel, M.M. (2002) Rb–Sr and Sm–Nd isotopic study of the Puquí complex, Colombian Andes. Journal of South American Earth Sciences, 15, 173–182.

Cawood, P.A. (2005) Terra Australis Orogen: Rodinia breakup and development of the Pacific and Iapetus margins of Gondwana during the Neoproterozoic and Paleozoic. Earth-Science Reviews, 69, 249–279.

Cawood, P.A., and Buchan, C. (2007) Linking accretionary orogenesis with supercontinent assembly. Earth-Science Reviews, 82, 217–256.

Cawood, P.A., Hawkesworth, C.J., and Dhuime, B. (2012) Detrital zircon record and tectonic setting. Geology, 40, 875–878.

Chapman, A.D., Saleeby, J.B., Wood, D.J., Piasecki, A., Kidder, S., Ducea, M.N., and Farley, K.A. (2012) Late Cretaceous gravitational collapse of the southern Sierra Nevada batholith, California. Geosphere, 8, 314–341.

Chapman, A.D., Saleeby, J.B., and Eiler, J. (2013) Slab flattening trigger for isotopic disturbance and magmatic flare-up in the southernmost Sierra Nevada batholith, California. Geology, 41, 1007–1010.

Chapman, J.B., Ducea, M.N., DeCelles, P.G., and Profeta, L. (2015) Tracking changes in crustal thickness during orogenic evolution with Sr/Y: An example from the North American Cordillera. Geology, 43, 919–922.

Cembrano, J., Lavenu, A., Reynolds, P., and Arancibia, G. (2002) Late Cenozoic transpressional ductile deformation north of the Nazca–South America–Antarctica triple junction. Tectonophysics, 354, 289–314.

Centeno-García, E. (2005) Review of Upper Paleozoic and Lower Mesozoic stratigraphy and depositional environments of central and west Mexico: Constraints on terrane analysis and paleogeography. In T.H. Anderson, J.A. Nourse, J.W. McKee, and M.B. Steiner, Eds., The Mojave-Sonora megashear hypothesis Development, assessment, and alternatives. Geological Society of America Special Paper 393, pp. 233–258.

Centeno-García, E., Busby, C., Busby, M., and Gehrels, G. (2011) Evolution of the Guerrero composite terrane along the Mexican margin, from extensional fringing arc to contractional continental arc. Geological Society of America Bulletin, 123, 1776–1797.

Centeno-García, E., Ruiz, J., Coney, P.J., Patchett, P.J., and Ortega-Gutiérrez, F. (1993) Guerrero terrane of Mexico: Its role in the Southern Cordillera from new geochemical data. Geology, 21, 419–422.

Chapman, A.D., Ducea, M.N., Kidder, S., and Petrescu, L. (2014) Geochemical constraints on the petrogenesis of the Salinian arc, central California: Implications for the origin of intermediate magmas. Lithos, 200-201, 126–141.

Chaussard, E., and Amelung, F. (2014) Regional controls on magma ascent and storage in volcanic arcs. Geochemistry, Geophysics, Geosystems, 15, 1407–1418.

Chen, J.H., and Moore, J.G. (1982) Uranium-lead isotopic ages from the Sierra Nevada Batholith, California. Journal of Geophysical Research, 87, 4761–4784.

Chernicoff, C.J., Zappettini, E.O., Santos, J.O., McNaughton, N.J., and Belousova, E. (2013) Combined U-Pb SHRIMP and Hf isotope study of the Late Paleozoic Yaminué Complex, Rio Negro Province, Argentina: Implications for the origin and evolution of the Patagonia composite terrane. Geoscience Frontiers, 4, 37–56.

Chew, D.M., Schaltegger, U., Košler, J., Whitehouse, M.J., Gutjahr, M., Spikings, R.A., and Miskovic, A. (2007) U-Pb geochronologic evidence for the evolution of the Gondwanan margin of the north-central Andes. Geological Society of America Bulletin, 119, 697–711.

Chiaradia, M. (2015) Crustal thickness control on Sr/Y signatures of recent arc magmas: an Earth scale perspective. Scientific Reports, 5, 8115.

Chin, E.J., Lee, C.-T.A., and Blichert-Toft, J. (2015) Growth of upper plate lithosphere controls tempo of arc magmatism: Constraints from Al-diffusion kineticsand coupled Lu-Hf and Sm-Nd chronology. Geochemical Perspectives Letters, 1, 20–32.

Clift, P., and Vannucchi, P. (2004) Controls on tectonic accretion versus erosion in subduction zones: Implications for the origin and recycling of the continental crust. Reviews of Geophysics, 42, RG2001.

Cochrane, R., Spikings, R., Gerdes, A., Ulianov, A., Mora, A., Villagómez, D., Putlitz, B., and Chiaradia, M. (2014) Permo-Triassic anatexis, continental rifting and the disassembly of western Pangaea. Lithos, 190-191, 383–402.

Cocks, L.R.M., and Torsvik, T.H. (2002) Earth geography from 500 to 400 million years ago: a faunal and palaeomagnetic review. Journal of the Geological Society, London, 159, 631–644.

Collins, W.J. (2002) Hot orogens, tectonic switching, and creation of continental crust. Geology, 30, 535–538.

Collo, G., Astini, R.A., Cawood, P.A., Buchan, C., and Pimentel, M. (2009) U–Pb detrital zircon ages and Sm–Nd isotopic features in low-grade metasedimentary rocks of the Famatina belt: implications for late Neoproterozoic–early Palaeozoic evolution of the proto-Andean margin of Gondwana. Journal of the Geological Society, 166, 303–319.

Colpron, M., and Nelson, J.L. (2011) A Palaeozoic NW passage and the Timanian, Caledonian and Uralian connections of some exotic terranes in the North American Cordillera. In A.M. Spencer, A.F. Embry, D.L. Gautier, A.V. Stoupakova, and K. Sørensen, Eds., Arctic Petroleum Geology: Geological Society, London, Memoirs 35, pp. 463–484.

Colpron, M., and Nelson, J.L. (2009) A Palaeozoic Northwest Passage: incursion of Caledonian, Baltican and Siberian terranes into eastern Panthalassa, and the early evolution of the North American Cordillera. In P.A. Cawood and A. Kröner, Eds., Earth accretionary systems in space and time. Geological Society, London, Special Publications 318, pp. 273–307.

Condie, K.C., Belousova, E., Griffin, W.L., and Sircombe, K.N. (2009) Granitoid events in space and time: Constraints from igneous and detrital zircon age spectra. Gondwana Research, 15, 228–242.

Condie, K.C., Bickford, M.E., Aster, R.C., Belousova, E., and Scholl, D.W. (2011) Episodic zircon ages, Hf isotopic composition, and the preservation rate of continental crust. Geological Society of America Bulletin, 123, 951–957.

Crisp, J.A. (1984) Rates of magma emplacement and volcanic output. Journal of Volcanology and Geothermal Research, 20, 177–211.

Crowley, Q.G., Key, R., and Noble, S.R. (2015) High-precision U–Pb dating of complex zircon from the Lewisian Gneiss Complex of Scotland using an incremental CA-ID-TIMS approach. Gondwana Research, 27, 1381–1391.

Dahlquist, J.A., Alasino, P.H., and Bello, C. (2013) Devonian F-rich peraluminous A-type magmatism in the proto-Andean foreland (Sierras Pampeanas, Argentina): geochemical constraints and petrogenesis from the western-central region of the Achala batholith. Mineralogy and Petrology, 108, 391–417.

Davidson, J.P., and Arculus, R. (2006) The significance of Phanerozoic arc magmatism in generating continental crust. In M. Brown and T. Rushmer, Eds., Evolution and Differentiation of the Continental Crust, pp. 135-172. Cambridge University Press.

Davis, G.A., Monger, J.W.H., and Burchfiel, B.C. (1978) Mesozoic construction of the Cordilleran “collage,” central British Columbia to central California. In D.G. Howell, and K.A. McDougall, Eds., Mesozoic Paleogeography of the Western United States. Los Angeles, California, Pacific Section, Society of Economic Paleontologists and Mineralogists, Pacific Coast Paleogeography Symposium 2, p. 1–32.

de Silva, S. (2008) Arc magmatism, calderas, and supervolcanoes. Geology, 36, 671–672.

de Silva, S., Zandt, G., Trumbull, R., Viramonte, J.G., Salas, G., and Jimenez, N. (2006) Large ignimbrite eruptions and volcano-tectonic depressions in the Central Andes: a thermomechanical perspective. In C. Troise, G. De Natale, and C.R.J. Kilburn, Eds., Mechanisms of activity and unrest at large calderas: Geological Society, London, Special Publication 269, pp. 47–63.

de Silva, S.L., and Gosnold, W.D. (2007) Episodic construction of batholiths: Insights from the spatiotemporal development of an ignimbrite flare-up. Journal of Volcanology and Geothermal Research, 167, 320–335.

de Silva, S.L., Riggs, N.R., and Barth, A.P. (2015) Quickening the pulse: fractal tempos in continental arc magmatism. Elements, 11, 113–118.

DeCelles, P.G., Ducea, M.N., Kapp, P., and Zandt, G. (2009) Cyclicity in Cordilleran orogenic systems. Nature Geoscience, 2, 251–257.

DeCelles, P.G., Zandt, G., Beck, S.L., Currie, C.A., Ducea, M.N., Kapp, P., Gehrels, G.E., Carrapa, B., and Quade, J. (2015) Cyclical orogenic processes in the Cenozoic central Andes. In P.G. DeCelles, M.N. Ducea, B. Carrapa, and P.A. Kapp, Eds., Geodynamics of a Cordilleran Orogenic System: The Central Andes of Argentina and Northern Chile. Geological Society of America Memoir 212, pp. 459–490.

Defant, M.J., and Drummond, M.S. (1990) Derivation of some modern arc magmas by melting of young subducted lithosphere. Nature, 347, 662–665.

Defant, M.J., and Kepezhinskas, P. (2001) Evidence suggests slab melting in arc magmas. Eos Transactions, American Geophysical Union, 82, 65–69.

Demouy, S., Paquette, J.-L., de Saint Blanquat, M., Benoit, M., Belousova, E.A., O'Reilly, S.Y., García, F., Tejada, L.C., Gallegos, R., and Sempere, T. (2012) Spatial and temporal evolution of Liassic to Paleocene arc activity in southern Peru unraveled by zircon U–Pb and Hf in-situ data on plutonic rocks. Lithos, 155, 183–200.

DePaolo, D.J. (1981a) A neodymium and strontium isotopic study of the mesozoic calc-alkaline granitic batholiths of the sierra Nevada and Peninsular Ranges, California. Journal of Geophysical Research, 86, 470–488.

DePaolo, D.J. (1981b) Trace element and isotopic effects of combined wallrock assimilation and fractional crystallization. Earth and Planetary Science Letters, 53, 189–202.

DePaolo, D.J., and Wasserburg, G.J. (1979) Petrogenetic mixing models and Nd-Sr isotopic patterns. Geochimica et Cosmochimica Acta, 43, 615–627.

Dewey, J.F., and Bird, J.M. (1970) Mountain belts and the new global tectonics. Journal of Geophysical Research, 75, 2625–2647.

Dickinson, W.R. (1970) Global Tectonics. Science, 168, 1250–1258.

Dickinson, W.R. (2004) Evolution of the North American Cordillera. Annual Review of Earth and Planetary Science Letters, 32, 13–45.

Dickinson, W.R. (2009) Anatomy and global context of the North American Cordillera. In S. Mahlburg Kay, V.A. Ramos, and W.R. Dickinson, Eds., Backbone of the Americas: shallow subduction, plateau uplift, and ridge and terrane collision. Geological Society of America Memoirs 204, pp. 1–29.

Dickinson, W.R., and Lawton, T.F. (2001) Carboniferous to Cretaceous assembly and fragmentation of Mexico. Geological Society of America Bulletin, 113, 1142–1160.

Dickinson, W.R., and Snyder, W.S. (1978) Plate tectonics of the Laramide orogeny. In V. Matthews III, Ed., Laramide folding associated with basement block faulting in the western United States. Geological Society of America Memoirs 151, pp. 355–366.

Dodson, M.H., Compston, W., Williams, I.S., and Wilson, J.F. (1988) A search for ancient detrital zircons in Zimbabwean sediments. Journal of the Geological Society, 145, 977–983.

Dowe, D.S., Nance, R.D., Keppie, J.D., Cameron, K.L., Ortega-Rivera, A., Ortega-Gutiérrez, F., and Lee, J.W.K. (2005) Deformational history of the Granjeno Schist, Ciudad Victoria, Mexico: Constraints on the closure of the Rheic Ocean? International Geology Review, 47, 920–937.

du Bray, E.A., and John, D.A. (2011) Petrologic, tectonic, and metallogenic evolution of the Ancestral Cascades magmatic arc, Washington, Oregon, and northern California. Geosphere, 7, 1102–1133.

Ducea, M. (2001) The California arc: Thick granitic batholiths, eclogitic residues, lithospheric-scale thrusting, and magmatic flare-ups. GSA Today, 11, 4–10.

Ducea, M.N. (2011) Fingerprinting orogenic delamination. Geology, 39, 191–192.

Ducea, M.N., and Barton, M.D. (2007) Igniting flare-up events in Cordilleran arcs. Geology, 35, 1047.

Ducea, M.N., Kidder, S., and Zandt, G. (2003) Arc composition at mid-crustal depths: Insights from the Coast Ridge Belt, Santa Lucia Mountains, California. Geophysical Research Letters, 30, 1703.

Ducea, M.N., Paterson, S.R., and DeCelles, P.G. (2015) High-Volume Magmatic Events in Subduction Systems. Elements, 11, 107–112.

Dufek, J., and Bergantz, G.W. (2005) Lower Crustal Magma Genesis and Preservation: a Stochastic Framework for the Evaluation of Basalt-Crust Interaction. Journal of Petrology, 46, 2167–2195.

Eagles, G. (2007) New angles on South Atlantic opening. Geophysical Journal International, 168, 353–361.

Eagles, G., Gohl, K., and Larter, R.D. (2004) High-resolution animated tectonic reconstruction of the South Pacific and West Antarctic Margin. Geochemistry, Geophysics, Geosystems, 5, Q07002.

Elías-Herrera, M., and Ortega-Gutiérrez, F. (2002) Caltepec fault zone: An Early Permian dextral transpressional boundary between the Proterozoic Oaxacan and Paleozoic Acatlán complexes, southern Mexico, and regional tectonic implications. Tectonics, 21, 1–19.

Elkins Tanton, L., Grove, T.L., and Donnelly-Nolan, J. (2001) Hot, shallow mantle melting under the Cascades volcanic arc. Geology, 29, 631–634.

Engebretson, D.C., Cox, A., and Gordon, R.G. (1985) Relative Motions Between Oceanic and Continental Plates in the Pacific Basin. In D.C. Engebretson, A. Cox, and R.G. Gordon, Eds., Relative motions between oceanic and continental plates in the Pacific basin. Geological Society of America Special Paper 206, pp. 1–60.

England, P., and Wilkins, C. (2004) A simple analytical approximation to the temperature structure in subduction zones. Geophysical Journal International, 159, 1138–1154.

England, P., Engdahl, R., and Thatcher, W. (2004) Systematic variation in the depths of slabs beneath arc volcanoes. Geophysical Journal International, 156, 377–408.

England, P.C., and Katz, R.F. (2010) Melting above the anhydrous solidus controls the location of volcanic arcs. Nature, 467, 700–703.

Fastovsky, D.E., Hermes, O.D., Strater, N.H., Bowring, S.A., Clark, J.M., Montellano, M., and Rene, H.R. (2005) Pre–Late Jurassic, fossil-bearing volcanic and sedimentary red beds of Huizachal Canyon, Tamaulipas, Mexico. In T.H. Anderson, J.A. Nourse, J.W. McKee, and M.B. Steiner, Eds., The Mojave-Sonora Megashear hypothesis: development, assessment, and alternatives. Geological Society of America Special Paper 393, pp. 401–426.

Ferrari, L., López-Martínez, M., Aguirre-Díaz, G., and Carrasco-Núñez, G. (1999) Space-

This is a preprint, the final version is subject to change, of the American Mineralogist (MSA)
Cite as Authors (Year) Title. American Mineralogist, in press.
(DOI will not work until issue is live.) DOI: http://dx.doi.org/10.2138/am-2016-5718

time patterns of Cenozoic arc volcanism in central Mexico: from the Sierra Madre Occidental to the Mexican Volcanic Belt. Geology, 27, 303–306.

Galaz, G., Keppie, J.D., Lee, J.K.W., and Ortega-Rivera, A. (2013) A high-pressure folded klippe at Tehuitzingo on the western margin of an extrusion zone, Acatlán Complex, southern México. Gondwana Research, 23, 641–660.

Gehrels, G.E., Dickinson, W.R., Riley, B.C.D., Finney, S.C., and Smith, M.T. (2000) Detrital zircon geochronology of the Roberts Mountains allochthon, Nevada. In M.J. Soreghan and G.E. Gehrels, Eds., Paleozoic and Triassic paleogeography and tectonics of western Nevada and Northern California. Geological Society of America Special Papers 347, pp. 19–42.

Gehrels, G., Rusmore, M., Woodsworth, G., Crawford, M., Andronicos, C., Hollister, L., Patchett, J., Ducea, M., Butler, R., Klepeis, K., and others (2009) U-Th-Pb geochronology of the Coast Mountains batholith in north-coastal British Columbia: Constraints on age and tectonic evolution. Geological Society of America Bulletin, 121, 1341–1361.

Gill, J.B. (1981) Orogenic andesites and plate tectonics, 390 p. Springer, Berlin.

Godínez-Urban, A., Lawton, T.F., Molina-Garza, R.S., Iriondo, A., Weber, B., and López-Martínez, M. (2011) Jurassic volcanic and sedimentary rocks of the La Silla and Todos Santos Formations, Chiapas: Record of Nazas arc magmatism and rift-basin formation prior to opening of the Gulf of Mexico. Geosphere, 7, 121–144.

Gosen, Von, W., and Prozzi, C. (1998) Structural evolution of the Sierra de San Luis (Eastern Sierras Pampeanas, Argentina): implications for the Proto-Andean Margin of Gondwana. In R.J. Pankhurst and C.W. Rapela, Eds., The Proto-Andean Margin of Gondwana. Geological Society of London Special Publications 142, pp. 235–258.

Grajales-Nishimura, J.M., Centeno-García, E., Keppie, J.D., and Dostal, J. (1999) Geochemistry of Paleozoic basalts from the Juchatengo complex of southern Mexico: tectonic implications. Journal of South American Earth Sciences, 12, 537–544.

Gromet, P., and Silver, L.T. (1987) REE variations across the Peninsular Ranges Batholith: Implications for batholithic petrogenesis and crustal growth in magmatic arcs. Journal of Petrology, 28, 75–125.

Gutscher, M., Spakman, W., Bijwaard, H., and Engdahl, E. (2000) Geodynamics of flat subduction: seismicity and tomographic constraints from the Andean margin. Tectonics, 19, 814–833.

Haschke, M. (2002) Repeated crustal thickening and recycling during the Andean orogeny in north Chile (21°–26° S). Journal of Geophysical Research, 107, 2019.

Haschke, M., Günther, A., Melnick, D., Echtler, H., Reutter, K.-J., Scheuber, E., and Oncken, O. (2006) Central and Southern Andean Tectonic Evolution Inferred from

Arc Magmatism. In O. Oncken, Ed., The Andes: Active Subduction Orogeny, pp. 337–353. Springer.

Haeussler, P.J., Bradley, D.C., Wells, R.E., and Miller, M.L. (2003) Life and death of the Resurrection plate: Evidence for its existence and subduction in the northeastern Pacific in Paleocene–Eocene time. Geological Society of America Bulletin, 115, 867–880.

Hawkesworth, C., Cawood, P., and Dhuime, B. (2013) Continental growth and the crustal record. Tectonophysics, 609, 651–660.

Hawkesworth, C., Cawood, P., Kemp, T., Storey, C., and Dhuime, B. (2009) A Matter of Preservation. Science, 323, 49–50.

Hawkesworth, C.J., Dhuime, B., Pietranik, A.B., Cawood, P.A., Kemp, A.I.S., and Storey, C.D. (2010) The generation and evolution of the continental crust. Journal of the Geological Society, London, 167, 229–248.

Hawkesworth, C.J., Gallagher, K., Hergt, J.M., and McDermott, F. (1993) Mantle and slab contributions in arc magmas. Annual Review of Earth and Planetary Science Letters, 21, 175–204.

Hebert, L.B., Antoshechkina, P., and Asimow, P. (2009) Emergence of a low-viscosity channel in subduction zones through the coupling of mantle flow and thermodynamics. Earth and Planetary Science Letters, 278, 243–256.

Heine, C., Zoethout, J., and Müller, R.D. (2013) Kinematics of the South Atlantic rift. Solid Earth Discussions, 5, 41–116.

Helbig, M., Keppie, J.D., Murphy, J.B., and Solari, L.A. (2012a) Exotic rifted passive margin of a back-arc basin off western Pangea: geochemical evidence from the Early Mesozoic Ayú Complex, southern Mexico. International Geology Review, 1–19.

Helbig, M., Keppie, J.D., Murphy, J.B., and Solari, L.A. (2012b) U-Pb geochronological constraints on the Triassic–Jurassic Ayú Complex, southern Mexico: Derivation from the western margin of Pangea-A. Gondwana Research, 22, 910–927.

Hervé, F., Calderón, M., Fanning, C.M., and Pankhurst, R.J. (2013) Provenance variations in the Late Paleozoic accretionary complex of central Chile as indicated by detrital zircons. Gondwana Research, 23, 1122–1135.

Hervé, F., Fanning, C.M., Calderón, M., and Mpodozis, C. (2014) Early Permian to Late Triassic batholiths of the Chilean Frontal Cordillera (28°–31° S): SHRIMP U–Pb zircon ages and Lu–Hf and O isotope systematics. Lithos, 184-187, 436–446.

Hervé, F., Pankhurst, R.J., Fanning, C.M., Calderón, M., and Yaxley, G.M. (2007) The South Patagonian batholith: 150 my of granite magmatism on a plate margin. Lithos, 97, 373–394.

Hildebrand, R.S., and Whalen, J.B. (2014a) Arc and slab-failure magmatism in Cordilleran Batholiths I–The Cretaceous Coastal Batholith of Peru and its role in South American orogenesis and hemispheric subduction flip. Geoscience Canada, 41, 255–282.

Hildebrand, R.S., and Whalen, J.B. (2014b) Arc and Slab-Failure Magmatism in Cordilleran Batholiths II – The Cretaceous Peninsular Ranges Batholith of Southern and Baja California. Geoscience Canada, 41, 399–458.

Hildreth, W., and Moorbath, S. (1988) Crustal contributions to arc magmatism in the Andes of Central Chile. Contributions to Mineralogy and Petrology, 98, 455–489.

Hughes, G.R., and Mahood, G.A. (2008) Tectonic controls on the nature of large silicic calderas in volcanic arcs. Geology, 36, 627.

Huppert, H.E., and Sparks, R.S.J. (1988) The Generation of Granitic Magmas by Intrusion of Basalt into Continental Crust. Journal of Petrology, 29, 599–624.

Iwamori, H. (1998) Transportation of H_2O and melting in subduction zones. Earth and Planetary Science Letters, 160, 65–80.

Jackson, J., and Molnar, P. (1990) Active faulting and block rotations in the western Transverse ranges, California. Journal of Geophysical Research, 95, 22073–22022.

Jackson, M.D., Cheadle, M.J., and Atherton, M.P. (2003) Quantitative modeling of granitic melt generation and segregation in the continental crust. Journal of Geophysical Research, 108, 2332.

Jagoutz, O.E. (2010) Construction of the granitoid crust of an island arc. Part II: a quantitative petrogenetic model. Contributions to Mineralogy and Petrology, 160, 359–381.

Jicha, B.R., and Jagoutz, O. (2015) Magma Production Rates for Intraoceanic Arcs. Elements, 11, 99–105.

Jones, R.E., Kirstein, L.A., Kasemann, S.A., and Dhuime, B. (2015) Geodynamic controls on the contamination of Cenozoic arc magmas in the southern Central Andes: Insights from the O and Hf isotopic composition of zircon. Geochimica et Cosmochimica Acta, 164, 386–402.

Karlstrom, K.E., Miler, C.F., Kingsbury, J.A., and Wooden, J.L. (1993) Pluton emplacement along an active ductile thrust zone, Piute Mountains, southeastern California: Interaction between deformational and solidifcation processes. Geological Society of America Bulletin, 105, 213–230.

Karlstrom, L., Lee, C.A., and Manga, M. (2014) The role of magmatically driven lithospheric thickening on arc front migration. Geochemistry, Geophysics, Geosystems, 15, 2655–2675.

Kato, T.T., Sharp, W.D., and Godoy, E. (2008) Inception of a Devonian subduction zone along the southwestern Gondwana margin: 40Ar– 39Ar dating of eclogite–amphibolite assemblages in blueschist boulders from the Coastal Range of Chile (41° S). Canadian Journal of Earth Sciences, 45, 337–351.

Kay, R.W. (1978) Aleutian magnesian andesites: melts from subducted Pacific Ocean crust. Journal of Volcanology and Geothermal Research, 4, 117–132.

Kay, R.W., and Mahlburg Kay, S. (1993) Delamination and delamination magmatism. Tectonophysics, 219, 177–189.

Keppie, D.F. (2015) How the closure of paleo-Tethys and Tethys oceans controlled the early breakup of Pangaea. Geology, 43, 335–338.

Keppie, J.D. (2004) Terranes of Mexico revisited: A 1.3 billion year odyssey. International Geology Review, 46, 765–794.

Keppie, J.D., Dostal, J., Miller, B.V., Ortega-Rivera, A., Roldán-Quintana, J., and Lee, J.W.K. (2006) Geochronology and geochemistry of the Francisco Gneiss: Triassic continental rift tholeiites on the Mexican margin of Pangea metamorphosed and exhumed in a Tertiary core complex. International Geology Review, 48, 1–16.

Keppie, J.D., Dostal, J., Murphy, J.B., and Galaz-Escanilla, G. (2012) High pressure rocks of the Acatlán Complex, southern Mexico: Large-scale subducted Ordovician rifted passive margin extruded into the upper plate during the Devonian–Carboniferous. Tectonophysics, 560-561, 1–21.

Keppie, J.D., Dostal, J., Murphy, J.B., and Nance, R.D. (2008) Synthesis and tectonic interpretation of the westernmost Paleozoic Variscan orogen in southern Mexico: From rifted Rheic margin to active Pacific margin. Tectonophysics, 461, 277–290.

Keppie, J.D., Nance, R.D., Ramos-Arias, M.A., Lee, J.K.W., Dostal, J., Ortega-Rivera, A., and Murphy, J.B. (2010) Late Paleozoic subduction and exhumation of Cambro-Ordovician passive margin and arc rocks in the northern Acatlán Complex, southern Mexico: Geochronological constraints. Tectonophysics, 495, 213–229.

Kerr, A.C., Aspden, J.A., Tarney, J., and Pilatasig, L.F. (2002) The nature and provenance of accreted oceanic terranes in western Ecuador: geochemical and tectonic constraints. Journal of the Geological Society, 159, 577–594.

Kidder, S., Ducea, M., Gehrels, G., Patchett, P.J., and Vervoort, J. (2003) Tectonic and magmatic development of the Salinian Coast Ridge Belt, California. Tectonics, 22, TC1409.

Kirsch, M., Helbig, M., Keppie, J.D., Murphy, J.B., Lee, J.K.W., and Solari, L.A. (2014) A Late Triassic tectonothermal event in the eastern Acatlan Complex, southern Mexico, synchronous with a magmatic arc hiatus: The result of flat-slab subduction? Lithosphere, 6, 63–79.

Kirsch, M., Keppie, J.D., Murphy, J.B., and Lee, J.K.W. (2013) Arc plutonism in a transtensional regime: the late Palaeozoic Totoltepec pluton, Acatlán Complex, southern Mexico. International Geology Review, 55, 263–286.

Kirsch, M., Keppie, J.D., Murphy, J.B., and Solari, L.A. (2012) Permian–Carboniferous arc magmatism and basin evolution along the western margin of Pangea: geochemical and geochronological evidence from the eastern Acatlán Complex, southern Mexico. Geological Society of America Bulletin, 124, 1607–1628.

Kistler, R.W., Wooden, J.L., Premo, W.R., and Morton, D.M. (2014) Pb-Sr-Nd-O isotopic characterization of Mesozoic rocks throughout the northern end of the Peninsular Ranges batholith: Isotopic evidence for the magmatic evolution of oceanic arc–continental margin accretion during the Late Cretaceous of southern California. In D.M. Morton and F.K. Miller, Eds., Peninsular Ranges Batholith, Baja California and Southern California. Geological Society of America Memoir 211, pp. 263–316.

Klemetti, E.W., and Clynne, M.A. (2014) Localized Rejuvenation of a Crystal Mush Recorded in Zircon Temporal and Compositional Variation at the Lassen Volcanic Center, Northern California. PLoS ONE, 9, e113157.

König, S., Schuth, S., Münker, C., and Qopoto, C. (2006) The role of slab melting in the petrogenesis of high-Mg andesites: evidence from Simbo Volcano, Solomon Islands. Contributions to Mineralogy and Petrology, 153, 85–103.

Laya, J.C., and Tucker, M.E. (2012) Facies analysis and depositional environments of Permian carbonates of the Venezuelan Andes: Palaeogeographic implications for Northern Gondwana. Palaeogeography, Palaeoclimatology, Palaeoecology, 331-332, 1–26.

Lee, C.-T.A., and Anderson, D.L. (2015) Continental crust formation at arcs, the arclogite “delamination” cycle, and one origin for fertile melting anomalies in the mantle. Science Bulletin, 1–16.

Lee, C.A., Shen, B., Slotnick, B.S., Liao, K., Dickens, G.R., Yokoyama, Y., Lenardic, A., Dasgupta, R., Jellinek, M., Lackey, J.S., and others (2013) Continental arc-island arc fluctuations, growth of crustal carbonates, and long-term climate change. Geosphere, 9, 21–36.

Leeman, W.P. (1983) The influence of crustal structure on compositions of subduction-related magmas. Journal of Volcanology and Geothermal Research, 18, 561–588.

Leeman, W.P. (1996) Boron and Other Fluid-mobile Elements in Volcanic Arc Lavas: Implications for Subduction Processes. In G.E. Bebout, D.W. Scholl, S.H. Kirby, and J.P. Platt, Eds., Subduction Top to Bottom. Geophysical Monograph 96, pp. 269–276. American Geophysical Union, Washington, D. C.

Lima, S.M., Corfu, F., Neiva, A.M.R., and Ramos, J.M.F. (2012) Dissecting Complex Magmatic Processes: an in-depth U-Pb Study of the Pavia Pluton, Ossa-Morena

Zone, Portugal. Journal of Petrology, 53, 1887–1911.

Lipman, P.W. (1992) Magmatism in the Cordilleran United States; progress and problems. In B.C. Burchfiel, P.W. Lipman, and M.L. Zoback, Eds., The Cordilleran orogen: conterminous U.S. pp. 481–514. Geological Society of America, Boulder, Colorado.

Litherland, M., Aspden, J.A., and Jemielita, R.A. (1994) The metamorphic belts of Ecuador, British Geological Survey, Overseas Memoir 11, 174p.

Loewy, S.L., Connelly, J.N., and Dalziel, I.W.D. (2004) An orphaned basement block: The Arequipa-Antofalla Basement of the central Andean margin of South America. Geological Society of America Bulletin, 116, 171–183.

Lomb, N.R. (1976) Least-squares frequency analysis of unequally spaced data. Astrophysics and Space Science, 39, 447–462.

Luyendyk, B.P., Kamerling, M.J., and Terres, R. (1980) Geometric model for Neogene crustal rotations in southern California. Geological Society of America Bulletin, 91, 211–217.

Madsen, J.K., Thorkelson, D.J., Friedman, R.M., and Marshall, D.D. (2006) Cenozoic to Recent plate configurations in the Pacific Basin: Ridge subduction and slab window magmatism in western North America. Geosphere, 2, 11–24.

Mahlburg Kay, S., and Mpodozis, C. (2001) Central Andean ore deposits linked to evolving shallow subduction systems and thickening crust. GSA Today, 11, 4–9.

Mahoney, J.B., Gordee, S.M., Haggart, J.W., Friedman, R.M., Diakow, L.J., and Woodsworth, G.J. (2009) Magmatic evolution of the eastern Coast Plutonic Complex, Bella Coola region, west-central British Columbia. Geological Society of America Bulletin, 121, 1362–1380.

Maksaev, V., Munizaga, F., and Tassinari, C. (2014) Timing of the magmatism of the paleo-Pacific border of Gondwana: U-Pb geochronology of Late Paleozoic to Early Mesozoic igneous rocks of the north Chilean Andes between 20° and 31° S. Andean Geology, 41, 447–506–506.

Mamani, M., Wörner, G., and Sempere, T. (2010) Geochemical variations in igneous rocks of the Central Andean orocline (13 S to 18 S): Tracing crustal thickening and magma generation through time and space. Geological Society of America Bulletin, 122, 162–182.

Mantle, G.W., and Collins, W.J. (2008) Quantifying crustal thickness variations in evolving orogens: Correlation between arc basalt composition and Moho depth. Geology, 36, 87–90.

Martini, M., Ferrari, L., López-Martínez, M., and Valencia, V. (2010) Stratigraphic redefinition of the Zihuatanejo area, southwestern Mexico. Revista Mexicana de Ciencias Geológicas, 27, 412–430.

Martini, M., Mori, L., Solari, L., and Centeno-García, E. (2011) Sandstone provenance of the Arperos Basin (Sierra de Guanajuato, central Mexico): Late Jurassic–Early Cretaceous back-Arc spreading as the foundation of the Guerrero Terrane. The Journal of Geology, 119, 597–617.

Martini, M., Solari, L., and Camprubí, A. (2013) Kinematics of the Guerrero terrane accretion in the Sierra de Guanajuato, central Mexico: new insights for the structural evolution of arc–continent collisional zones. International Geology Review, 55, 574–589.

Matthews, K.J., Seton, M., and Müller, R.D. (2012) A global-scale plate reorganization event at 105−100Ma. Earth and Planetary Science Letters, 355–356, 283–298.

Matzel, J.E.P., Bowring, S.A., and Miller, R.B. (2006) Time scales of pluton construction at differing crustal levels: Examples from the Mount Stuart and Tenpeak intrusions, North Cascades, Washington. Geological Society of America Bulletin, 118, 1412–1430.

Matzel, J.E.P., Bowring, S.A., and Miller, R.B. (2004) Protolith age of the Swakane Gneiss, North Cascades, Washington: Evidence of rapid underthrusting of sediments beneath an arc. Tectonics, 23, TC6009.

Matzel, J.E.P., Bowring, S.A., and Miller, R.B. (2008) Spatial and temporal variations in Nd isotopic signatures across the crystalline core of the North Cascades, Washington. In J.E. Wright and J.W. Shervais, Eds., Ophiolites, Arcs, and Batholiths A Tribute to Cliff Hopson. Geological Society of America Special Papers 438, pp. 499–516.

McGeary, S., Nur, A., and Ben-Avraham, Z. (1985) Spatial gaps in arc volcanism: The effect of collision or subduction of oceanic plateaus. Tectonophysics, 119, 195–221.

Memeti, V., Paterson, S.R., and Putirka, K.D. (2014) Formation of the Sierra Nevada Batholith: Magmatic and tectonic processes and their tempos: Geological Society of America Field Guides 34. (V. Memeti, S.R. Paterson, & K.D. Putirka, Eds.).

Miller, E.L., Miller, M.M., Stevens, C.H., Wright, J.E., and Madrid, R.J. (1992) Late Paleozoic paleogeographic and tectonic evolution of the western U.S. Cordillera. In B.C. Burchfiel, P.W. Lipman, and M.L. Zoback, Eds., The Cordilleran orogen: conterminous U.S., pp. 57–106. Geological Society of America, Boulder, Colorado.

Miller, R.B., Haugerud, R.A., Murphy, F., and Nicholson, L.S. (1994) Tectonostratigraphic framework of the northeastern Cascades. Washington Division of Geology and Earth Resources Bulletin, 80, 73–92.

Miller, R.B., Paterson, S.R., and Matzel, J.P. (2009) Plutonism at different crustal levels: Insights from the ~5–40 km (paleodepth) North Cascades crustal section, Washington. In R.B. Miller and A.W. Snoke, Eds., Crustal cross sections from the western North American Cordillera and elsewhere implications for tectonic and petrologic processes. Geological Society of America Special Paper 456, pp. 125–149.

Mišković, A., Spikings, R.A., Chew, D.M., Košler, J., Ulianov, A., and Schaltegger, U. (2009) Tectonomagmatic evolution of Western Amazonia: Geochemical characterization and zircon U-Pb geochronologic constraints from the Peruvian Eastern Cordilleran granitoids. Geological Society of America Bulletin, 121, 1298–1324.

Monger, J., and Price, R. (2002) The Canadian Cordillera: Geology and tectonic evolution. CSEG Recorder, 17, 17–36.

Monger, J.W.H., Price, R.A., and Tempelman-Kluit, D.J. (1982) Tectonic accretion and the origin of the two major metamorphic and plutonic welts in the Canadian Cordillera. Geology, 10, 70–75.

Montecinos, P., Schärer, U., Vergara, M., and Aguirre, L. (2008) Lithospheric Origin of Oligocene-Miocene Magmatism in Central Chile: U-Pb Ages and Sr-Pb-Hf Isotope Composition of Minerals. Journal of Petrology, 49, 555–580.

Morton, D.M., Miller, F.K., Kistler, R.W., Premo, W.R., Lee, C.A., Langenheim, V.E., Wooden, J.L., Snee, L.W., Clausen, B.L., and Cossette, P. (2014) Framework and petrogenesis of the northern Peninsular Ranges batholith, southern California. In D.M. Morton and F.K. Miller, Eds., Peninsular Ranges Batholith, Baja California and Southern California. Geological Society of America Memoir 211, pp. 61–143.

Mukasa, S.B. (1986) Zircon U-Pb ages of super-units in the Coastal batholith, Peru: Implications for magmatic and tectonic processes. Geological Society of America Bulletin, 97, 241–254.

Mukasa, S.B., and Henry, D.J. (1990) The San Nicolas batholith of coastal Peru: early Palaeozoic continental arc or continental rift magmatism? Journal of the Geological Society, London, 147, 27–39.

Murphy, J.B., and Nance, R.D. (2008) The Pangea conundrum. Geology, 36, 703–706.

Müller, R.D., Dutkiewicz, A., Seton, M., and Gaina, C. (2013) Seawater chemistry driven by supercontinent assembly, breakup, and dispersal. Geology, 41, 907–910.

Nance, R.D., Gutierrez-Alonso, G., Keppie, J.D., Linnemann, U., Murphy, J.B., Quesada, C., Strachan, R.A., and Woodcock, N.H. (2012) A brief history of the Rheic Ocean. Geoscience Frontiers, 3, 125–135.

Nance, R.D., Murphy, J.B., and Santosh, M. (2014) The supercontinent cycle: A retrospective essay. Gondwana Research, 25, 4–29.

Nelson, J.L., Colpron, M., Piercey, S.J., Dusel-Bacon, C., Murphy, D.C., and Roots, C.F.

(2006) Paleozoic tectonic and metallogenetic evolution of pericratonic terranes in Yukon, northern British Columbia and eastern Alaska. In M. Colpron and J.L. Nelson, Eds., Paleozoic Evolution and Metallogeny of Pericratonic Terranes at the Ancient Pacific Margin of North America Vol. 45, pp. 323–360.

Nicholson, C., Sorlien, C.C., Atwater, T., Crowell, J.C., and Luyendyk, B.P. (1994) Microplate capture, rotation of the western Transverse Ranges, and initiation of the San Andreas transform as a low-angle fault system. Geology, 22, 491–495.

Nokleberg, W.J., Parfenov, L.M., Monger, J.W.H., Norton, I.O., Khanchuk, A.I., Stone, D.B., Scotese, C.R., Scholl, D.W., and Fujita, K. (2000) Phanerozoic tectonic evolution of the Circum-North Pacific. US Geological Survey Professional Paper, 1–102.

Oliveros, V., Labbé, M., Rossel, P., and Charrier, R. (2012) Late Jurassic paleogeographic evolution of the Andean back-arc basin: New constrains from the Lagunillas Formation, northern Chile (27° 30□–28° 30□S). Journal of South American Earth Sciences, 37, 25–40.

Ortega-Obregón, C., Solari, L., Gómez-Tuena, A., Elías-Herrera, M., Ortega-Gutiérrez, F., and Macías-Romo, C. (2014) Permian–Carboniferous arc magmatism in southern Mexico: U–Pb dating, trace element and Hf isotopic evidence on zircons of earliest subduction beneath the western margin of Gondwana. International Journal of Earth Sciences, 103, 1287–1300.

Otamendi, J.E., Ducea, M.N., and Bergantz, G.W. (2012) Geological, Petrological and Geochemical Evidence for Progressive Construction of an Arc Crustal Section, Sierra de Valle Fertil, Famatinian Arc, Argentina. Journal of Petrology, 53, 761–800.

Otamendi, J.E., Ducea, M.N., Tibaldi, A.M., Bergantz, G.W., la Rosa, de, J.D., and Vujovich, G.I. (2009) Generation of tonalitic and dioritic magmas by coupled partial melting of gabbroic and metasedimentary rocks within the deep crust of the Famatinian magmatic arc, Argentina. Journal of Petrology, 50, 841–873.

Palacios-García, N.B., and Martini, M. (2014) From back-arc rifting to arc accretion: the Late Jurassic–Early Cretaceous evolution of the Guerrero terrane recorded by a major provenance change in sandstones from the Sierra de los Cuarzos area, central Mexico. International Geology Review, 56, 1377–1394.

Pankhurst, R.J., Rapela, C.W., and Fanning, C.M. (2000) Age and origin of coeval TTG, I- and S-type granites in the Famatinian belt of NW Argentina. Transactions of the Royal Society of Edinburgh: Earth Sciences, 91, 151–168.

Pankhurst, R.J., Rapela, C.W., Fanning, C.M., and Márquez, M. (2006) Gondwanide continental collision and the origin of Patagonia. Earth-Science Reviews, 76, 235–257.

Pankhurst, R.J., Weaver, S.D., Hervé, F., and Larrondo, P. (1999) Mesozoic-Cenozoic evolution of the North Patagonian batholith in Aysen, southern Chile. Journal of the Geological Society, London, 156, 673–694.

Pardo Casas, F., and Molnar, P. (1987) Relative motion of the Nazca (Farallon) and South American Plates since Late Cretaceous time. Tectonics, 6, 233–248.

Paterson, S.R., and Ducea, M.N. (2015) Arc Magmatic Tempos: Gathering the Evidence. Elements, 11, 91–98.

Paterson, S.R., Memeti, V., Anderson, L., Cao, W., Lackey, J.S., Putirka, K.D., Miller, R.B., Miller, J.S., and Mundil, R. (2014) Overview of arc processes and tempos. In V. Memeti, S.R. Paterson, and K.D. Putirka, Eds., Formation of the Sierra Nevada Batholith: Magmatic and tectonic processes and their tempos: Geological Society of America Field Guides 34, pp. 87–116.

Paterson, S.R., Okaya, D., Memeti, V., Economos, R., and Miller, R.B. (2011) Magma addition and flux calculations of incrementally constructed magma chambers in continental margin arcs: Combined field, geochronologic, and thermal modeling studies. Geosphere, 7, 1439–1468.

Paterson, S.R., Clausen, B., and Kirsch, M. (2016), Exploring causes of Mesozoic arc flare-ups in the Peninsular Ranges Batholith, southern California. Geological Society of America 112th Cordilleran Section Annual Meeting, Ontario, CA, United States, 4–6 April 2016, abstract number 274397.

Peacock, S.M. (1990) Fluid processes in subduction zones. Science, 248, 329–337.

Pearce, J.A., Harris, N.B.W., and Tindle, A.G. (1984) Trace element discrimination diagrams for the tectonic interpretation of granitic rocks. Journal of Petrology, 25, 956–983.

Petford, N., and Gallagher, K. (2001) Partial melting of mafic (amphibolitic) lower crust by periodic influx of basaltic magma. Earth and Planetary Science Letters, 193, 483–499.

Pilger, R.H., Jr (1984) Cenozoic plate kinematics, subduction and magmatism: South American Andes. Journal of the Geological Society, 141, 793–802.

Pindell, J., Maresch, W.V., Martens, U., and Stanek, K. (2012) The Greater Antillean Arc: Early Cretaceous origin and proposed relationship to Central American subduction mélanges: implications for models of Caribbean evolution. International Geology Review, 54, 131–143.

Pindell, J.L., and Kennan, L. (2009) Tectonic evolution of the Gulf of Mexico, Caribbean and northern South America in the mantle reference frame: an update. In K.H. James, M.A. Lorente, and J.L. Pindell, Eds., The origin and evolution of the Caribbean plate. Geological Society, London, Special Publications 328, pp. 1–55.

Pitcher, W.S., Atherton, M.P., Cobbing, E.J., and Beckinsale, R.D. (1985) Magmatism at a Plate Edge: the Peruvian Andes, 387 p. Halsted Press, New York.

Plank, T., Cooper, L.B., and Manning, C.E. (2009) emerging geothermometers for estimating slabsurface temperatures. Nature Geoscience, 2, 611–615.

Premo, W.R., Morton, D.M., Wooden, J.L., and Fanning, C.M. (2014) U-Pb zircon geochronology of plutonism in the northern Peninsular Ranges batholith, southern California: Implications for the Late Cretaceous tectonic evolution of southern California. In D.M. Morton and F.K. Miller, Eds., Peninsular Ranges Batholith, Baja California and Southern California. Geological Society of America Memoir 211, pp. 145–180.

Proenza, J.A., Ortega-Gutiérrez, F., Camprubi, A., Trilla, J., Elías-Herrera, M., and Reyes-Salas, M. (2004) Paleozoic serpentinite-enclosed chromitites from Tehuitzingo (Acatlán Complex, southern Mexico): a petrological and mineralogical study. Journal of South American Earth Sciences, 16, 649–666.

Profeta, L., Ducea, M.N., Chapman, J.B., Paterson, S.R., Gonzales, S.M.H., Kirsch, M., Petrescu, L., and DeCelles, P.G. (2015) Quantifying crustal thickness overtime in magmatic arcs. Scientific Reports, 5, 17786.

Ramos, V.A. (2009) Anatomy and global context of the Andes: Main geologic features and the Andean orogenic cycle. In S. Mahlburg Kay, V.A. Ramos, and W.R. Dickinson, Eds., Backbone of the Americas: shallow subduction, plateau uplift, and ridge and terrane collision. Geological Society of America Memoirs 204, pp. 31–65.

Ramos, V.A. (2008) Patagonia: A paleozoic continent adrift? Journal of South American Earth Sciences, 26, 235–251.

Ramos, V.A. (2010) The Grenville-age basement of the Andes. Journal of South American Earth Sciences, 29, 77–91.

Ramos, V.A., and Aleman, A. (2000) Tectonic Evolution of the Andes. In U.G. Cordani, E.J. Milani, A. Thomaz Filho, and M.C. Campos Neto, Eds., Tectonic Evolution of South America pp. 635–685. Brazilian Academy of Science, Rio de Janeiro.

Ramos, V.A., and Naipauer, M. (2014) Patagonia: where does it come from? Journal of Iberian Geology, 40, 1–13.

Ramos-Arias, M.A., Keppie, J.D., Ortega-Rivera, A., and Lee, J.W.K. (2008) Extensional Late Paleozoic deformation on the western margin of Pangea, Patlanoaya area, Acatlán Complex, southern Mexico. Tectonophysics, 448, 60–76.

Rapalini, A.E., de Luchi, M., Dopico, C.M., and Klinger, F. (2010) Did Patagonia collide with Gondwana in the Late Paleozoic? Some insights from a multidisciplinary study of magmatic units of the North Patagonian Massif. Geologica Acta, 8, 349–371.

Rapela, C.W., and Pankhurst, R.J. (1992) The granites of northern Patagonia and the Gastre Fault System in relation to the break-up of Gondwana. In B.C. Storey, T. Alabaster, and R.J. Pankhurst, Eds., Magmatism and the causes of continental break-up. Geological Society, London, Special Publications 68, pp. 209–220.

Rapela, C.W., Pankhurst, R.J., Casquet, C., and Baldo, E. (1998a) Early evolution of the Proto-Andean margin of South America. Geology, 26, 707–710.

Rapela, C.W., Pankhurst, R.J., Casquet, C., Baldo, E., Saavedra, J., Galindo, C., and Fanning, C.M. (1998b) The Pampean Orogeny of the southern proto-Andes: Cambrian continental collision in the Sierras de Córdoba. In R.J. Pankhurst and C.W. Rapela, Eds., The Proto-Andean Margin of Gondwana. Geological Society, London, Special Publications 142, pp. 181–217.

Rapela, C.W., Verdecchia, S.O., Casquet, C., Pankhurst, R.J., Baldo, E.G., Galindo, C., Murra, J.A., Dahlquist, J.A., and Fanning, C.M. (2016) Identifying Laurentian and SW Gondwana sources in the Neoproterozoic to Early Paleozoic metasedimentary rocks of the Sierras Pampeanas: Paleogeographic and tectonic implications. Gondwana Research, 32, 193–212.

Reitsma, M.J. (2012) Reconstructing the Late Paleozoic - Early Mesozoic plutonic and sedimentary record of south-east Peru: Orphaned back-arcs along the western margin of Gondwana. (U. Schaltegger & R. Spikings, Eds.). Université de Genève, Genève.

Riley, B.C.D., Snyder, W.S., and Gehrels, G.E. (2000) U-Pb detrital zircon geochronology of the Golconda allochthon, Nevada. In M.J. Soreghan and G.E. Gehrels, Eds., Paleozoic and Triassic paleogeography and tectonics of western Nevada and Northern California. Geological Society of America Special Papers 347, pp. 65–75.

Rolando, A.P., Hartmann, L.A., Santos, J., Fernandez, R.R., Etcheverry, R.O., Schalamuk, I.A., and McNaughton, N.J. (2002) SHRIMP zircon U–Pb evidence for extended Mesozoic magmatism in the Patagonian Batholith and assimilation of Archean crustal components. Journal of South American Earth Sciences, 15, 267–283.

Romeuf, N., Aguirre, L., Soler, P., Feraud, G., Jaillard, E., and Ruffet, G. (1995) Middle Jurassic volcanism in the northern and central Andes. Andean Geology, 22, 245–259.

Rosenau, M., Melnick, D., and Echtler, H. (2006) Kinematic constraints on intra-arc shear and strain partitioning in the southern Andes between 38° S and 42° S latitude. Tectonics, 25, TC4013.

Rossel, P., Oliveros, V., Ducea, M.N., Charrier, R., Scaillet, S., Retamal, L., and Figueroa, O. (2013) The Early Andean subduction system as an analog to island arcs: Evidence from across-arc geochemical variations in northern Chile. Lithos, 179, 211–230.

Rudnick, R.L. (1995) Making continental crust. Nature, 378, 1–8.

Ruiz, G.M.H., Seward, D., and Winkler, W. (2007) Evolution of the Amazon Basin in Ecuador with Special Reference to Hinterland Tectonics: Data from Zircon Fission-Track and Heavy Mineral Analysis. In M.A. Mange and D.T. Wright, Eds., Heavy Minerals in Use Vol. 58, pp. 907–934. Elsevier.

Saleeby, J. (2003) Segmentation of the Laramide Slab - Evidence from the southern Sierra Nevada region. Geological Society of America Bulletin, 115, 655–668.

Saleeby, J., and Dunne, G. (2015) Temporal and tectonic relations of early Mesozoic arc magmatism, southern Sierra Nevada, California. In T.H. Anderson, A.N. Didenko, C.L. Johnson, A.I. Khanchuk, and J.H. MacDonald Jr., Eds., Late Jurassic Margin of Laurasia—A Record of Faulting Accommodating Plate Rotation. Geological Society of America Special Paper 513, doi:10.1130/2015.2513(05).

Scargle, J.D. (1982) Studies in astronomical time series analysis. II – statistical aspects of spectral analysis of unevenly spaced data. Astrophysical Journal, 263, 835–853.

Schaaf, P., Weber, B., Weis, P., Gross, A., Ortega-Gutiérrez, F., and Köhler, H. (2002) The Chiapas Massif (Mexico) revised: New geologic and isotopic data for basement characteristics. Neues Jahrbuch für Geologie und Paläontologie - Abhandlungen, 225, 1–23.

Schaltegger, U., Schmitt, A.K., and Horstwood, M. (2015) U–Th–Pb zircon geochronology by ID-TIMS, SIMS, and laser ablation ICP-MS: recipes, interpretations, and opportunities. Chemical Geology, 402, 89–110.

Scholl, D.W., and Huene, von, R. (2009) Implications of estimated magmatic additions and recycling losses at the subduction zones of accretionary (non-collisional) and collisional (suturing) orogens. In P.A. Cawood and A. Kröner, Eds., Earth accretionary systems in space and time. Geological Society, London, Special Publications 318, pp. 105–125.

Schweickert, R.A., and Cowan, D.S. (1975) Early Mesozoic tectonic evolution of the western Sierra Nevada, California. Geological Society of America Bulletin, 86, 1329–1336.

Scotese, C.R. (1997) The PALEOMAP Project: Paleogeographic atlas and plate tectonic software: Paleogeographic atlas and plate tectonic software. Department of Geology, University of Texas, Austin, USA.

Sdrolias, M., and Müller, R.D. (2006) Controls on back-arc basin formation. Geochemistry, Geophysics, Geosystems, 7, Q04016.

Sedlock, R.L., Ortega-Gutiérrez, F., and Speed, R.C. (1993) Tectonostratigraphic Terranes and Tectonic Evolution of Mexico, 153 p. Vol. 278, pp. 1–153. Geological Society of America Special Paper 278.

Sempere, T., Carlier, G., Soler, P., Fornari, M., Carlotto, V., Jacay, J., Arispe, O., Néraudeau, D., Cárdenas, J., and Rosas, S. (2002) Late Permian–Middle Jurassic lithospheric thinning in Peru and Bolivia, and its bearing on Andean-age tectonics. Tectonophysics, 345, 153–181.

Sempere, T., Folguera, A., and Gerbault, M. (2008) New insights into Andean evolution: An introduction to contributions from the 6th ISAG symposium (Barcelona, 2005). Tectonophysics, 459, 1–13.

Seton, M., Müller, R.D., Zahirovic, S., Gaina, C., Torsvik, T., Shephard, G., Talsma, A., Gurnis, M., Turner, M., Maus, S., and others (2012) Global continental and ocean basin reconstructions since 200Ma. Earth-Science Reviews, 113, 212–270.

Shephard, G.E., Müller, R.D., and Seton, M. (2013) The tectonic evolution of the Arctic since Pangea breakup: Integrating constraints from surface geology and geophysics with mantle structure. Earth-Science Reviews, 124, 148–183.

Silva-Romo, G., Arellano-Gil, J., Mendoza-Rosales, C., and Nieto-Obregón, J. (2000) A submarine fan in the Mesa Central, Mexico. Journal of South American Earth Sciences, 13, 429–442.

Silver, L.T., and Chappell, B.W. (1988) The Peninsular Ranges Batholith: an insight into the evolution of the Cordilleran batholiths of southwestern North America. Transactions of the Royal Society of Edinburgh: Earth Sciences, 79, 105–121.

Sircombe, K.N. (2000) Quantitative comparison of large sets of geochronological data using multivariate analysis: a provenance study example from Australia. Geochimica et Cosmochimica Acta, 64, 1593–1616.

Solari, L.A., Ortega-Gutiérrez, F., Elías-Herrera, M., Schaaf, P., Norman, M., Torres de León, R., Ortega-Obregón, C., Chiquin, M., and Morán-Ical, S. (2009) U-Pb zircon geochronology of Paleozoic units in Western and Central Guatemala: insights into the tectonic evolution of Middle America. In K.H. James, M.A. Lorente, and J. and Pindell, Eds., The origin and evolution of the Caribbean plate. Geological Society, London, Special Publications 328, pp. 293–311.

Somoza, R. (1998) Updated Nazca (Farallon)—South America relative motions during the last 40 My: implications for mountain building in the central Andean region. Journal of South American Earth Sciences, 11, 211–215.

Spikings, R., Cochrane, R., Villagómez, D., Van der Lelij, R., Vallejo, C., Winkler, W., and Beate, B. (2014) The geological history of northwestern South America: from Pangaea to the early collision of the Caribbean Large Igneous Province (290–75 Ma). Gondwana Research, 27, 95–139.

Spikings, R.A., Crowhurst, P.V., Winkler, W., and Villagómez, D. (2010) Syn- and post-accretionary cooling history of the Ecuadorian Andes constrained by their in-situ and detrital thermochronometric record. Journal of South American Earth Sciences, 30, 121–133.

Spikings, R.A., Winkler, W., Seward, D., and Handler, R. (2001) Along-strike variations in the thermal and tectonic response of the continental Ecuadorian Andes to the collision with heterogeneous oceanic crust. Earth and Planetary Science Letters, 186, 57–73.

Stampfli, G.M., and Borel, G.D. (2002) A plate tectonic model for the Paleozoic and Mesozoic constrained by dynamic plate boundaries and restored synthetic oceanic isochrons. Earth and Planetary Science Letters, 196, 17–33.

Stern, C.R. (2004) Active Andean volcanism: its geologic and tectonic setting. Revista geológica de Chile, 31, 161–206.

Stern, T.W., Bateman, P.C., Morgan, B.A., Newell, M.F., and Peck, D.L. (1981) Isotopic U-Pb ages of zircon from the granitoids of the central Sierra Nevada, California. Professional Paper 1185. United States Geological Survey.

Stevens, C.H., and Greene, D.C. (1999) Stratigraphy, depositional history, and tectonic evolution of Paleozoic continental-margin rocks in roof pendants of the eastern Sierra Nevada, California. Geological Society of America Bulletin, 111, 919–933.

Storey, B.C. (1995) The role of mantle plumes in continental breakup: case histories from Gondwanaland. Nature, 377, 301–308.

Tabor, R.W., Haugerud, R.A., Brown, E.H., Babcock, R.S., and Miller, R.B. (1989) Accreted Terranes of the North Cascades Range, Washington: Spokane to Seattle, Washington, July 21–29, 1989. American Geophysical Union, Washington, D. C.

Tatsumi, Y. (2005) The subduction factory: How it operates in the evolving Earth. GSA Today, 15, 4–10.

Tatsumi, Y., and Eggins, S. (1995) Subduction zone magmatism, 224 p. John Wiley and Sons Ltd, Oxford, United Kingdom.

Tatsumi, Y., and Stern, R.J. (2006) The subduction factory. Oceanography, 19, 1–9.

Taylor, G.K., Grocott, J., Pope, A., and Randall, D.E. (1998) Mesozoic fault systems, deformation and fault block rotation in the Andean forearc: a crustal scale strike-slip duplex in the Coastal Cordillera of northern Chile. Tectonophysics, 299, 93–109.

Telgársky, R. (2013) Dominant Frequency Extraction. A Computing Research Repository, arXiv:1306.0103vl, 1–12.

Torres, R., Ruiz, J., Patchett, P.J., and Grajales-Nishimura, J.M. (1999) Permo-Triassic continental arc in eastern Mexico; tectonic implications for reconstructions of southern North America. In C. Bartolini, J.L. Wilson, and T.F. Lawton, Eds., Mesozoic sedimentary and tectonic history of north-central Mexico. Geological

Society of America Special Paper 340, pp. 191–196.

Torsvik, T.H., Rousse, S., Labails, C., and Smethurst, M.A. (2009) A new scheme for the opening of the South Atlantic Ocean and the dissection of an Aptian salt basin. Geophysical Journal International, 177, 1315–1333.

Trumbull, R.B., Riller, U., Oncken, O., Scheuber, E., Munier, K., and Hongn, F. (2006) The Time-Space Distribution of Cenozoic Volcanism in the South-Central Andes: a New Data Compilation and Some Tectonic Implications. In O. Oncken, G. Chong, G. Franz, P. Giese, H.-J. Götze, V.A. Ramos, M.R. Strecker, and P. Wigger, Eds., The Andes pp. 29–43. Springer Berlin Heidelberg.

Turner, S.J., and Langmuir, C.H. (2015a) The global chemical systematics of arc front stratovolcanoes: Evaluating the role of crustal processes. Earth and Planetary Science Letters, 422, 182–193.

Turner, S.J., and Langmuir, C.H. (2015b) What processes control the chemical compositions of arc front stratovolcanoes? Geochemistry, Geophysics, Geosystems, 16, 1865–1893.

Valencia-Moreno, M., Ruiz, J., Barton, M.D., Patchett, P.J., Zürcher, L., Hodkinson, D.G., and Roldán-Quintana, J. (2001) A chemical and isotopic study of the Laramide granitic belt of northwestern Mexico: Identification of the southern edge of the North American Precambrian basement. Geological Society of America Bulletin, 113, 1409–1422.

Vallejo, C., Spikings, R.A., Luzieux, L., Winkler, W., Chew, D., and Page, L. (2006) The early interaction between the Caribbean Plateau and the NW South American Plate. Terra Nova, 18, 264–269.

Van Buer, N.J., and Miller, E.L. (2010) Sahwave Batholith, NW Nevada: Cretaceous arc flare-up in a basinal terrane. Lithosphere, 2, 423–446.

Van Buer, N.J., Miller, E.L., and Dumitru, T.A. (2009) Early Tertiary paleogeologic map of the northern Sierra Nevada batholith and the northwestern Basin and Range. Geology, 37, 371–374.

Van der Lelij, R., Spikings, R., Ulianov, A., and Chiaradia, M. (2016) Palaeozoic to Early Jurassic history of the northwestern corner of Gondwana, and implications for the evolution of the Iapetus, Rheic and Pacific Oceans. Gondwana Research, 31, 271–294.

Vaughan, A.P.M., and Pankhurst, R.J. (2008) Tectonic overview of the West Gondwana margin. Gondwana Research, 13, 150–162.

Vermeesch, P. (2004) How many grains are needed for a provenance study? Earth and Planetary Science Letters, 224, 441–451.

Vermeesch, P. (2012) On the visualisation of detrital age distributions. Chemical Geology, 312-313, 190–194.

Villagómez, D., and Spikings, R. (2013) Thermochronology and tectonics of the Central and Western Cordilleras of Colombia: Early Cretaceous–Tertiary evolution of the Northern Andes. Lithos, 160-161, 228–249.

Villagómez, D., Spikings, R., Magna, T., Kammer, A., Winkler, W., and Beltrán, A. (2011) Geochronology, geochemistry and tectonic evolution of the Western and Central cordilleras of Colombia. Lithos, 125, 875–896.

Weber, B., Iriondo, A., Premo, W.R., Hecht, L., and Schaaf, P. (2007) New insights into the history and origin of the southern Maya block, SE México: U-Pb-SHRIMP zircon geochronology from metamorphic rocks of the Chiapas massif. International Journal of Earth Sciences, 96, 253–269.

Wobbe, F., Gohl, K., Chambord, A., and Sutherland, R. (2012) Structure and breakup history of the rifted margin of West Antarctica in relation to Cretaceous separation from Zealandia and Bellingshausen plate motion. Geochemistry, Geophysics, Geosystems, 13, Q04W12.

Yogodzinski, G.M., Lees, J.M., Churikova, T.G., and Dorendorf, F. (2001) Geochemical evidence for the melting of subducting oceanic lithosphere at plate edges. Nature, 409, 500–504.

Zaffarana, C., Tommasi, A., Vauchez, A., and Gregoire, M. (2014) Microstructures and seismic properties of south Patagonian mantle xenoliths (Gobernador Gregores and Pali Aike). Tectonophysics, 621, 175–197.

Zavala-Monsiváis, A., Barboza-Gudiño, J.R., Valencia, V.A., Rodríguez-Hernández, S.E., and García-Arreola, M.E. (2009) Las sucesiónes volcánicas pre-Cretácicas en el noreste de México. GEOS Unión Geofísica Mexicana, 29, 53.

Zavala-Monsiváis, A., Barboza-Gudiño, J.R., Velasco-Tapia, F., and García-Arreola, M.E. (2012) Sucesión volcánica Jurásica en el área de Charcas, San Luis Potosí: Contribución al entendimiento del Arco Nazas en el noreste de México. Boletín de la Sociedad Geológica Mexicana, 64, 277–293.

Zellmer, G.F. (2008) Some first-order observations on magma transfer from mantle wedge to upper crust at volcanic arcs. In C. Annen and G.F. Zellmer, Eds., Dynamics of Crustal Magma Transfer, Storage and Differentiation. Geological Society, London, Special Publication 304, pp. 15–31.

Zellmer, G.F., and Annen, C. (2008) An introduction to magma dynamics. In C. Annen and G.F. Zellmer, Eds., Dynamics of Crustal Magma Transfer, Storage and Differentiation. Geological Society, London, Special Publication 304, pp. 1–13.

Zhang, J., Ma, C., and She, Z. (2012) An Early Cretaceous garnet-bearing metaluminous

A-type granite intrusion in the East Qinling Orogen, central China: Petrological, mineralogical and geochemical constraints. Geoscience Frontiers, 3, 635–646.

Figure captions

Figure 1. Igneous and detrital zircon U-Pb age spectra providing a temporal record of Cordilleran arc magmatism between 400 and 80 Ma. Individual diagrams include TIMS, LA-ICP-MS, SHRIMP, and SIMS age data presented as histograms with a 10 m.y. bin width and adaptive KDE functions (see text for details). For bedrock ages (BA), the number of analyses (*n*) given in each plot represents the number of crystallization ages, which are composite ages calculated from three or more single zircons. Exception: igneous ages from the Sierra Nevada represent single zircon ages. In detrital zircon spectra (DZ), *n* refers to ages of single zircon grains (or a domain therein). On the right hand side, a map shows the extent of defined arc sectors and sample locations. Geological map data from Bouysse et al. (2010). Abbreviations in the age plots are as follows: PR—Peninsular Ranges, TR—Transverse Ranges, Moj—Mojave Desert, N Mex—Northern Mexico, SE Mexico—Southeastern Mexico. See DR-1 for data sources.

Figure 2. (a) Color contour plot of composite KDE functions, highlighting the spatial and temporal distribution of age populations (i.e., magmatic arc activity) along the Cordilleran arc. Labels of y-axis indicate the latitudinal centers of each Cordilleran arc sector along an along-arc profile. Letters A–H refer to the following arc sectors from north to south: A—Coast Ranges, B—Sierra Nevada, C—Peninsular and Transverse Ranges, Mojave, and northern Mexico, D—Southeastern Mexico and Central America, E—Northern Andes, F—Peruvian Andes, G—South-Central Andes, H—Southern Andes. (b) Color contour plot showing results of a Fast Fourier Transform (FFT) based time

series analysis to evaluate periods of dominant frequencies in Cordilleran arc age data.

Figure 3. Comparison of geochronological (panel 1), geochemical (panels 2–6), and kinematic data (panels 7–9) for arc-related igneous rocks in the sectors of (a) the Sierra Nevada, (b) the Peninsular and Transverse Ranges, Mojave, and northern Mexico, and (c) southeastern Mexico and Central America. Diagonally hatched bands mark magmatic flare-up events, visually delineated on the basis of peaks in the age spectra. For geochemical data, individual data points are plotted (dots), along with median values ± 1σ (circles and grey bars) for a moving 10 m.y. average. For kinematic data, black dots are average values and grey envelopes represent minimum–maximum ranges from a set of three values extracted per arc domain. Note differing age range in (c). Abbreviations: BA—bedrock ages, DZ—detrital zircons, OConv.—orthogonal convergence rate, PDispl.—parallel displacement rate. For data sources see DR-1.

Figure 4. Compilation of kinematic data for the Cordilleran orogen for the time between 200 and 50 Ma. Letters A–H refer to the following arc sectors from north to south: A—Coast Ranges, B—Sierra Nevada, C—Peninsular and Transverse Ranges, Mojave, and northern Mexico, D—Southeastern Mexico and Central America, E—Northern Andes, F—Peruvian Andes, G—South-Central Andes, H—Southern Andes. Each diagram contains (1) kernel density estimates of combined bedrock and detrital zircon age data, (2) trench-orthogonal convergence rates and (3) trench-parallel displacement rates between down-going oceanic and upper continental plates, and (4) slab age. Black dots in 2–4 are average values and grey envelopes represent minimum–maximum ranges from a set of three values extracted per arc domain.

This is a preprint, the final version is subject to change, of the American Mineralogist (MSA)
Cite as Authors (Year) Title. American Mineralogist, in press.
(DOI will not work until issue is live.) DOI: http://dx.doi.org/10.2138/am-2016-5718

Figure 5. Covariance matrix showing Pearson correlation coefficients for parameters of magmatism and plate kinematics. Letters A–H refer to the following arc sectors from north to south: A—Coast Ranges, B—Sierra Nevada, C—Peninsular and Transverse Ranges, Mojave, and northern Mexico, D—Southeastern Mexico and Central America, E—Northern Andes, F—Peruvian Andes, G—South-Central Andes, H—Southern Andes. Red is strong positive correlation; blue is strong negative correlation.

Figure 6. Tectonic map showing the principal geologic features of southeastern Mexico and Central America (J. D. Keppie 2004; Dowe et al. 2005; Helbig et al. 2012b). Colored squares indicate the location and age of igneous rocks. Pie-charts show detrital zircon age populations between 400 and 80 Ma.

Figure 7. Effect of lag time on Pearson correlation coefficients between age composite and orthogonal convergence rate. Letters A–H refer to the following arc sectors from north to south: A—Coast Ranges, B—Sierra Nevada, C—Peninsular and Transverse Ranges, Mojave, and northern Mexico, D—Southeastern Mexico and Central America, E—Northern Andes, F—Peruvian Andes, G—South-Central Andes, H—Southern Andes. Arc sectors represented by bold lines show an increase in correlation coefficients with variable lag times.

This is a preprint, the final version is subject to change, of the American Mineralogist (MSA)
Cite as Authors (Year) Title. American Mineralogist, in press.
(DOI will not work until issue is live.) DOI: http://dx.doi.org/10.2138/am-2016-5718

Figure 1

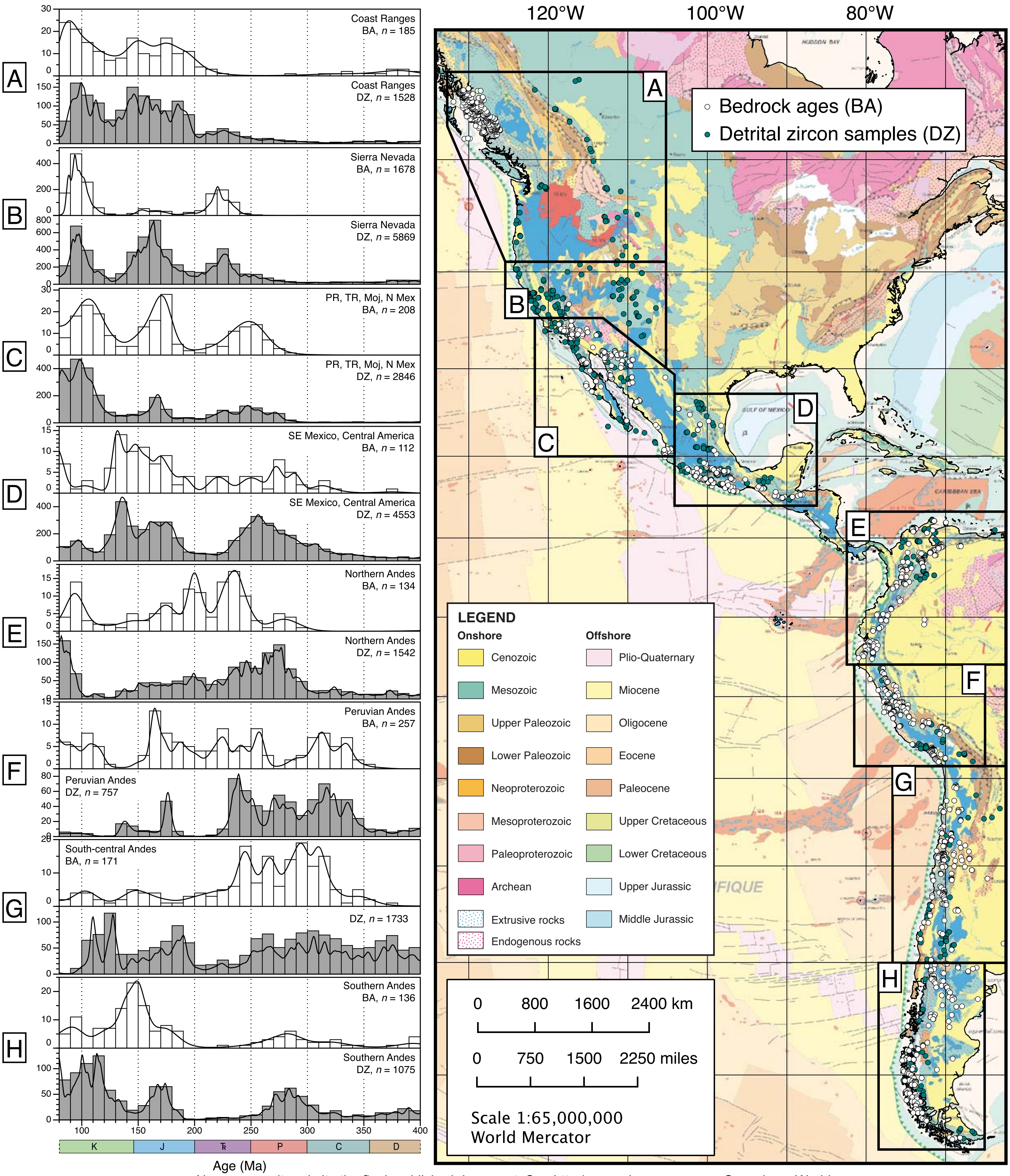

(DOI will not work until issue is live.) DOI: http://dx.doi.org/10.2138/am-2016-5718

Figure 2

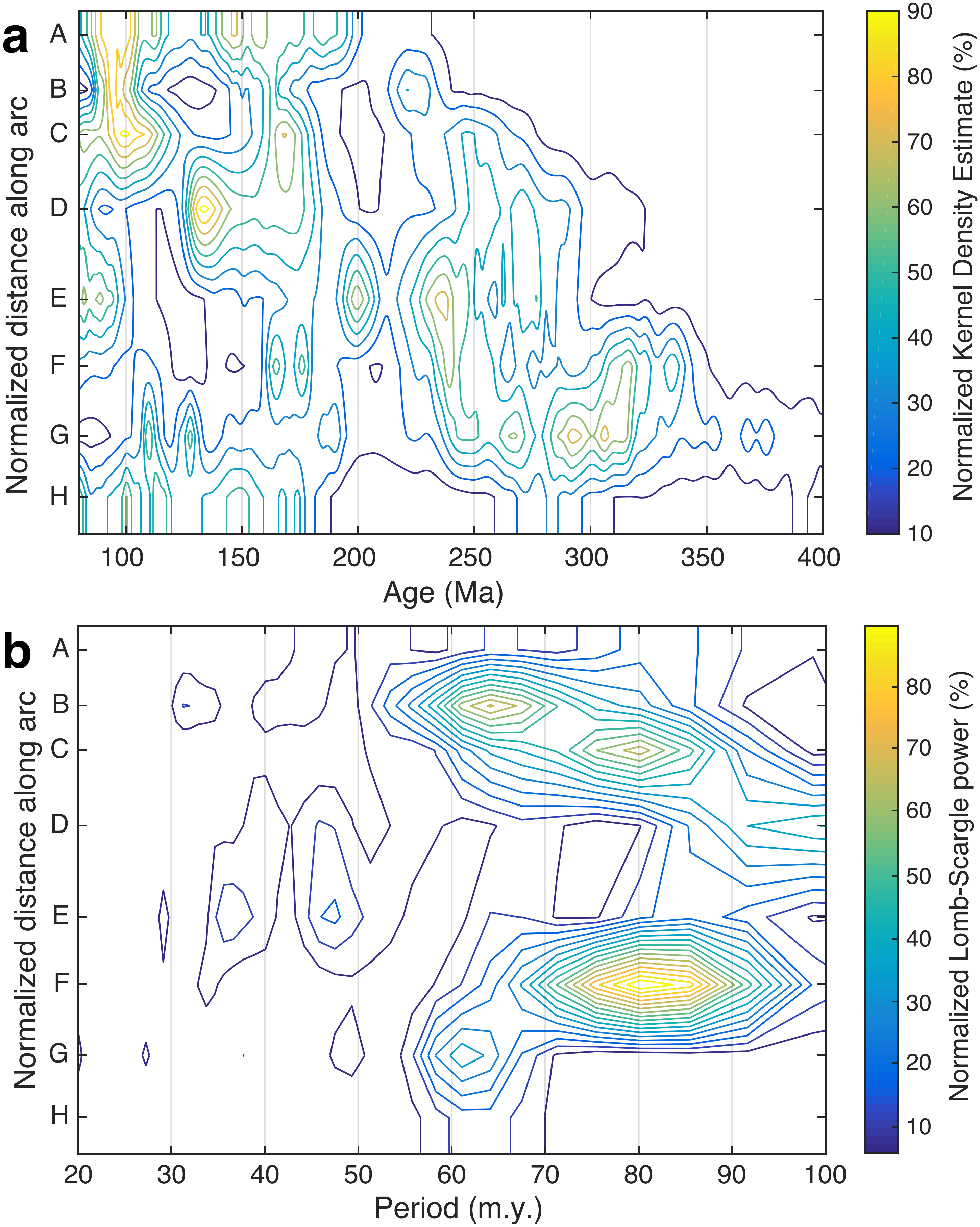

This is a preprint, the final version is subject to change, of the American Mineralogist (MSA)
Cite as Authors (Year) Title. American Mineralogist, in press.
(DOI will not work until issue is live.) DOI: http://dx.doi.org/10.2138/am-2016-5718

Figure 3

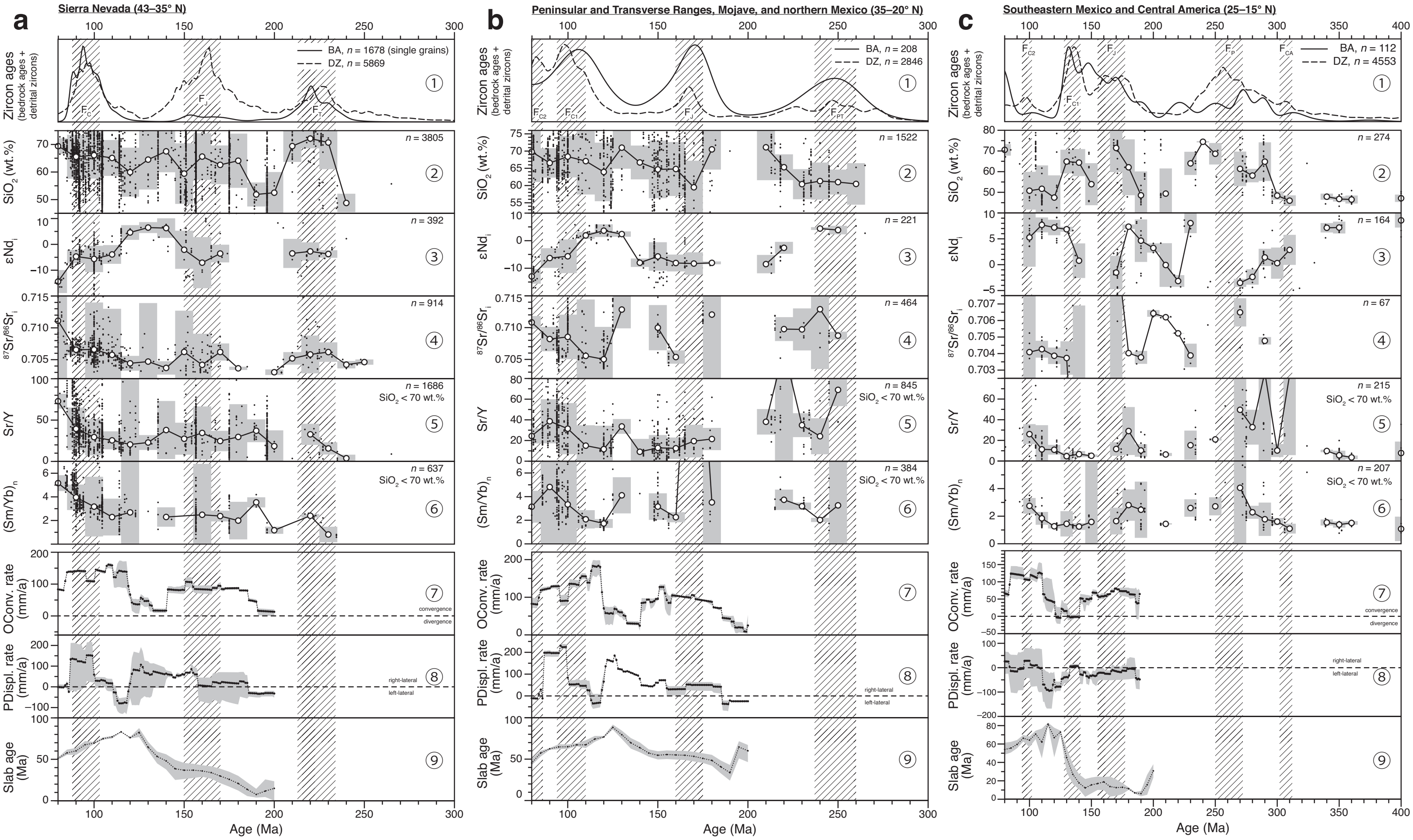

This is a preprint, the final version is subject to change, of the American Mineralogist (MSA)
Cite as Authors (Year) Title. American Mineralogist, in press.
(DOI will not work until issue is live.) DOI: http://dx.doi.org/10.2138/am-2016-5718

Figure 4

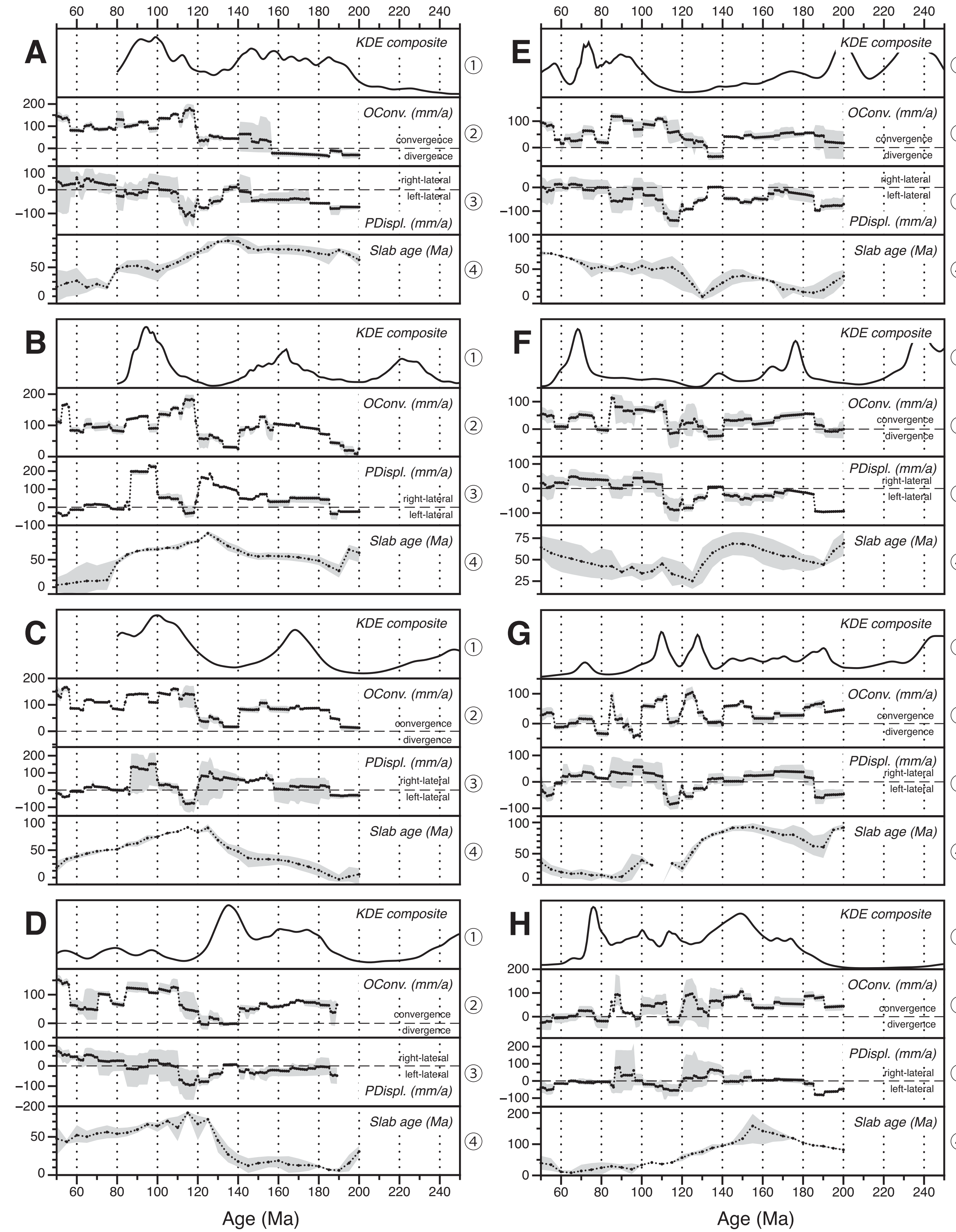

This is a preprint, the final version is subject to change, of the American Mineralogist (MSA)
Cite as Authors (Year) Title. American Mineralogist, in press.
(DOI will not work until issue is live.) DOI: http://dx.doi.org/10.2138/am-2016-5718

Figure 5

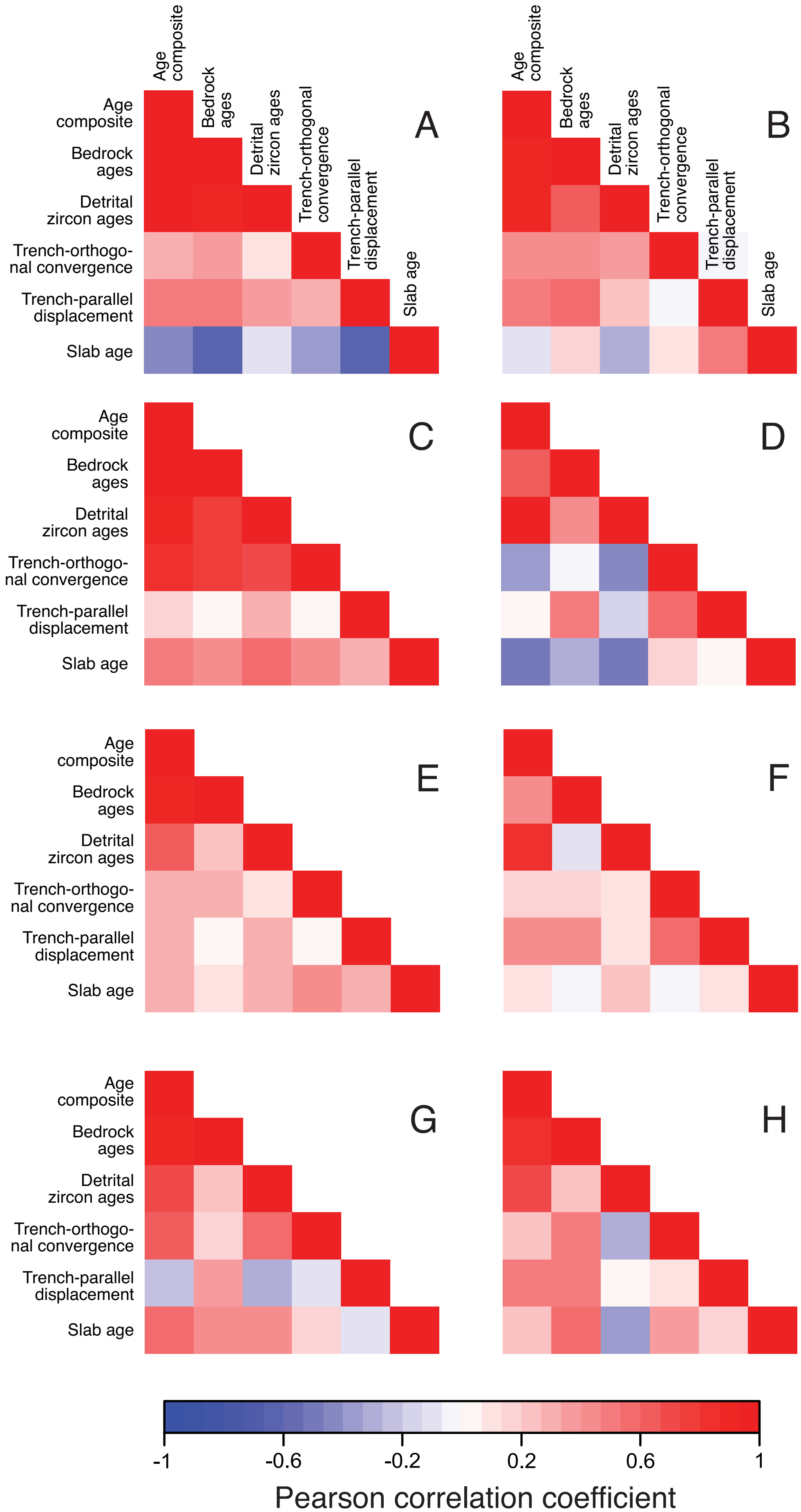

Figure 6

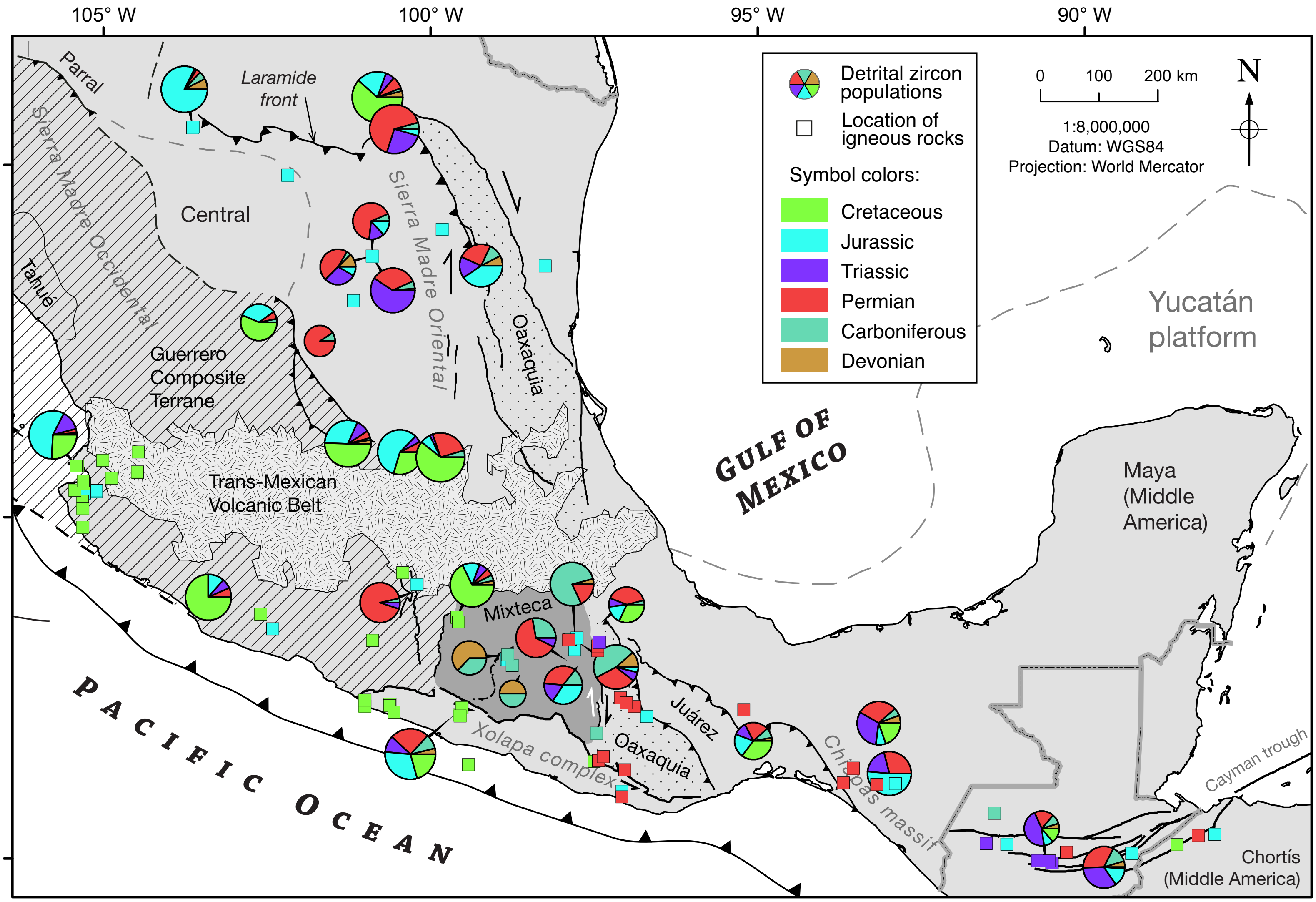
105° W
100° W
95° W
90° W
25° N
20° N
15° N
Detrital zircon populations
Location of igneous rocks
Symbol colors:
Cretaceous
Jurassic
Triassic
Permian
Carboniferous
Devonian
0
100
200 km
1:8,000,000
Datum: WGS84
Projection: World Mercator
N
Parral
Laramide front
Sierra Madre Occidental
Central
Tahué
Sierra Madre Oriental
Oaxaquia
Guerrero Composite Terrane
Trans-Mexican Volcanic Belt
Gulf of Mexico
Yucatán platform
Maya (Middle America)
Mixteca
Juárez
Oaxaquia
Xolapa complex
Chiapas massif
Cayman trough
Chortís (Middle America)
Pacific Ocean

Figure 7

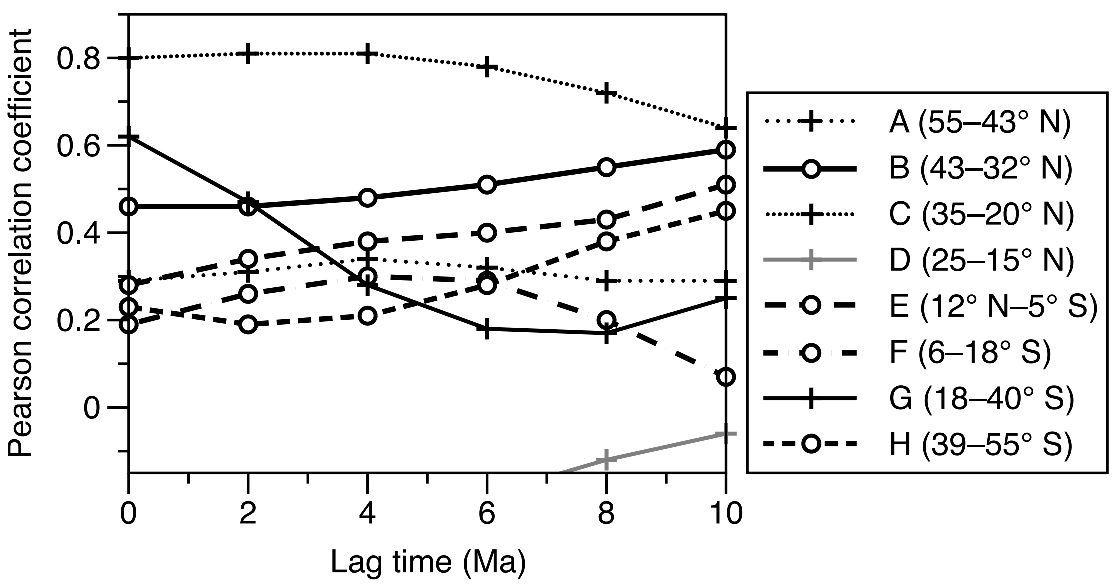
Pearson correlation coefficient
0.8
0.6
0.4
0.2
0
0
2
4
6
8
10
Lag time (Ma)
A (55–43° N)
B (43–32° N)
C (35–20° N)
D (25–15° N)
E (12° N–5° S)
F (6–18° S)
G (18–40° S)
H (39–55° S)